

InternAgent-1.5: A Unified Agentic Framework for Long-Horizon Autonomous Scientific Discovery

InternScience Team, Shanghai Artificial Intelligence Laboratory

⌚ <https://github.com/InternScience/InternAgent>

Artificial intelligence is rapidly emerging as a powerful engine for scientific discovery. Modern machine learning and large language models support literature analysis, hypothesis generation, experimental planning, and data interpretation across biology, chemistry, and earth science. These advances have inspired AI Scientist systems that coordinate computational modeling, laboratory experimentation, and cross disciplinary reasoning to accelerate scientific progress. However, existing AI Scientist systems remain limited by domain specific designs, incomplete reasoning abilities, naive optimization pipelines, and insufficient support for long horizon autonomous operation. We introduce InternAgent-1.5, a unified system designed for end-to-end scientific discovery across computational and empirical domains. The system is built on a structured architecture composed of three coordinated subsystems for generation, verification, and evolution. These subsystems are supported by foundational capabilities for deep research, solution optimization, and long horizon memory. The architecture allows InternAgent-1.5 to operate continuously across extended discovery cycles while maintaining coherent and improving behavior. It also enables the system to coordinate computational modeling and laboratory experimentation within a single unified system. We evaluate InternAgent-1.5 on scientific reasoning benchmarks such as GAIA, HLE, GPQA, and FrontierScience, and the system achieves leading performance that demonstrates strong foundational capabilities. Beyond these benchmarks, we further assess two categories of discovery tasks. In algorithm discovery tasks, InternAgent-1.5 autonomously designs competitive methods for core machine learning problems. In empirical discovery tasks, it executes complete computational or wet lab experiments and produces scientific findings in earth, life, biological, and physical domains. Overall, these results show that InternAgent-1.5 provides a general and scalable framework for autonomous scientific discovery.

Contents

1	Introduction	3
2	InternAgent-1.5	5
2.1	System Overview	5
2.1.1	Architecture	6
2.1.2	Foundational Capabilities	7
2.2	Cross Disciplinary Graph Construction and Knowledge Capturing	7
2.2.1	Cross-Disciplinary Knowledge Graph	7
2.2.2	Flow Graph	9
2.2.3	Graph-Guided Output Synthesis	9
2.3	Experiment Execution and Multi-round Parallel Optimization	10
2.3.1	Generative Design for Experimental Optimization	10
2.3.2	Scenario	11
2.4	Structured Cognitive Memory for Long Horizon Scientific Discovery	11
2.4.1	Strategy-Procedural Memory	12

2.4.2 Task-Episodic Memory	13
2.4.3 Semantic-Knowledge Memory	13
3 Experiments	13
3.1 Experiments Setup	13
3.1.1 General Scientific Reasoning Abilities	13
3.1.2 Algorithm Discovery	14
3.1.3 Empirical Discovery	15
3.2 Evaluating Agentic Reasoning Abilities	16
3.3 Results for Algorithm Discovery Tasks	18
3.3.1 Scientific Algorithm	18
3.3.2 AI Algorithm	20
3.4 Discoveries of Scientific Mechanism	21
3.4.1 Earth Science	21
3.4.2 Life Science	23
3.4.3 Biological Science	25
3.4.4 Physical Science	25
3.5 Effectiveness of Structured Cognitive Memory	27
4 Related Work	28
4.1 Agentic AI for Scientific Discovery	28
4.2 Deep Research Agents	29
4.3 Memory Mechanism	29
5 Conclusion	29
References	30
A Appendix	35
A.1 Contributions and Acknowledgments	35
A.2 Earth Science example	36

1. Introduction

Table 1 | Comparison with state-of-the-art frameworks for autonomous scientific discovery.

Method	Domains		Capabilities			
	Algorithm Discovery	Empirical Discovery	Deep Research	Solution Refinement	Wet Lab	Persistence Running
AI Scientist [1, 2]	✓	✗	✗	✓	✗	✗
AlphaEvolve [3]	✓	✗	✗	✓	✗	✗
AI Co-Scientist [4]	✗	✓	✓	✗	✓	✗
Robin [5]	✗	✓	✓	✗	✓	✗
Kosmos [6]	✗	✓	✓	✗	✓	✗
InternAgent 1.0 [7]	✓	✗	✗	✗	✗	✗
InternAgent 1.5	✓	✓	✓	✓	✓	✓

Artificial intelligence is rapidly reshaping the landscape of scientific research, giving rise to the emerging paradigm of AI for Science [8, 9]. Recent progress in machine learning has driven advances across biology [10, 11, 12], chemistry [13, 5], and the physical and environmental sciences [14]. Large language models have expanded this frontier by supporting literature analysis [15, 16], hypothesis generation [17, 18, 7], experimental planning [7, 19, 20], and data interpretation [21, 22]. These capabilities have motivated a shift toward autonomous scientific systems capable of coordinating complex workflows that span computational modeling, wet-lab experimentation, and cross-disciplinary reasoning.

A series of recent systems have demonstrated the potential of automated scientific agents. In algorithm optimization, AI Scientist [1, 2] and AlphaEvolve [3] integrate literature analysis, coding, and experimental evaluation into end-to-end research loops. In biomedicine, AI Co-Scientist [4] generates hypotheses and designs therapeutic experiments. In chemistry, systems such as ChemCrow [13] and Robin [5] connect large language models with domain specific toolchains for synthesis planning and molecular design. In earth science, EarthLink [14] integrates multisphere data and literature to support mechanism level reasoning. These systems have shown impressive domain-specific performance but operate as isolated verticals with architectures that embed strong domain assumptions. To move beyond single domain expertise, systems such as Kosmos [6] introduce structured scientific world models to organize research across metabolomics, materials science, and genetics.

Despite substantial progress, current systems of AI4S exhibit several characteristics that limit their ability to support autonomous cross-disciplinary discovery:

- **Domain-Specific Architectures:** Many systems are organized around discipline-focused designs, which makes it difficult to perform unified reasoning across scientific fields.
- **Partial Foundational Capabilities:** Existing frameworks vary in their support for the use of heterogeneous dry-lab and wet-lab experiments, leading to uneven coverage of core scientific competencies.
- **Linear Optimization Pipelines:** Optimization procedures are often based on trajectory-local updates and therefore do not integrate information across broader search processes when refining scientific proposals.
- **Limited Long-Horizon Operation:** Most systems do not maintain persistent memory over

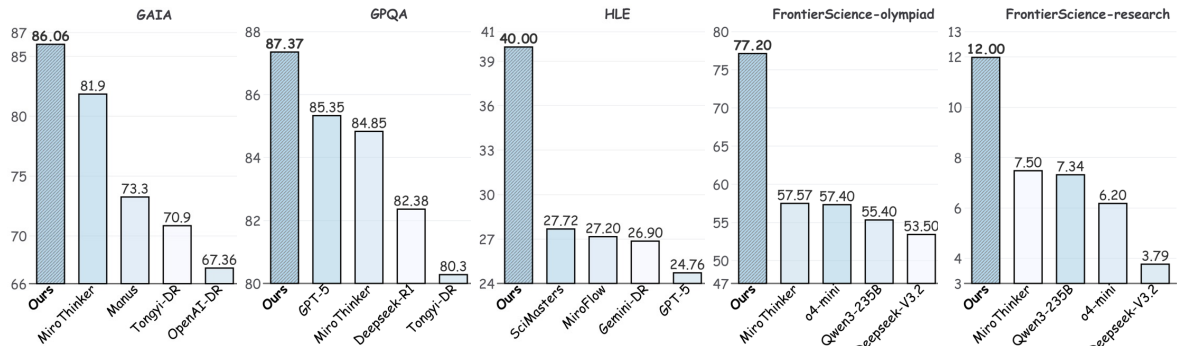


Figure 1 | Performance comparison of InternAgent-1.5 across GAIA [25], GPQA [26], HLE-full [27], and FrontierScience [28].

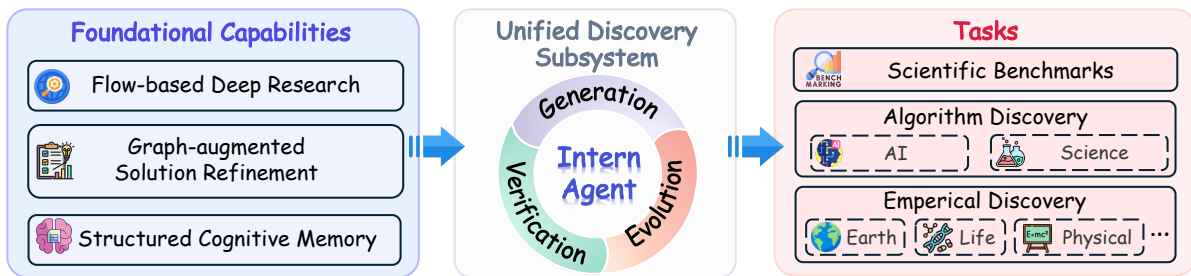


Figure 2 | Overview of InternAgent-1.5 that summarizes its foundational capabilities, unified discovery pipeline, and supported scientific tasks in a high-level manner.

extended research cycles, which restricts iterative refinement and long-term autonomous operation.

A comparative overview of existing systems is presented in Table 1, which summarizes these characteristics across domains and foundational capabilities.

To address these challenges, we adopt an epistemological perspective grounded in the philosophy of science [23, 24] and categorize tasks into two fundamental domains: **Algorithm Discovery**, which *transforms objectives into solutions in formal systems*, and **Empirical Discovery**, which *transforms observations into generalizations about the physical world*. A framework capable of supporting both domains requires unified architectural principles, strong foundational capabilities, long-horizon iterative optimization, and the ability to operate across computational and experimental environments.

Building on InternAgent 1.0 [7], we introduce InternAgent-1.5, a unified system designed for end-to-end scientific discovery. The system follows the observation that scientific inquiry across domains can be organized into a common structure that includes literature based hypothesis construction, methodological evaluation, and evidence driven refinement. InternAgent-1.5 operationalizes these processes through three coordinated subsystems, namely **Generation**, **Verification**, and **Evolution**. Each subsystem is driven by a foundational capability: *deep research* supports the **Generation** subsystem, *solution refinement* supports the **Verification** subsystem, and *long horizon memory* supports the **Evolution** subsystem. This design moves beyond structures restricted to single domain algorithm discovery and establishes a general framework suitable for both computational and empirical scientific tasks. A high level overview of InternAgent-1.5, including its core capabilities, subsystem organization, and supported discovery tasks, is presented in Fig. 2.

InternAgent-1.5 is evaluated across standard benchmarks and open ended scientific discovery tasks. The system attains leading performance on agentic reasoning abilities, demonstrating the effectiveness of the foundational capabilities that drive the Generation and Verification subsystems. These capabilities, together with long horizon memory in the Evolution subsystem, support stable extended operation and enable consistent iterative refinement throughout long discovery cycles. Building on this capability structure, InternAgent-1.5 further performs competitively in both **algorithm discovery** and **empirical discovery** tasks, indicating that the unified framework scales from benchmark level reasoning to practical scientific workflows.

In summary, the main contributions of this work are as follows:

- **A Unified Architecture for End-to-end Scientific Discovery:** InternAgent-1.5 organizes the scientific discovery process into three coherent subsystems for Generation, Verification, and Evolution. These subsystems support the full cycle of hypothesis formulation, methodological evaluation, and evidence driven refinement through foundational capabilities for deep research, solution refinement, and long horizon memory. This organization provides a robust basis for reliable and scalable scientific discovery.
- **State-of-the-Art Foundational Capabilities:** InternAgent-1.5 delivers strong foundational capabilities in deep research and solution refinement, supported by structured long horizon memory. Across benchmarks that measure cross disciplinary retrieval, structured reasoning, and scientifically grounded problem solving, the system achieves leading performance on HLE [27], GAIA [25], GPQA [26], FrontierScience [28], and SGI bench [29]. These results confirm that the foundational capabilities of InternAgent-1.5 are sufficiently reliable to support complex scientific workflows.
- **Sustained Autonomous Optimization:** InternAgent-1.5 integrates a structured memory architecture with an iterative optimization process centered on the Verification and Evolution subsystems. This design supports the accumulation of contextual knowledge, the sustained refinement of hypotheses, and the stable improvement of methodological plans across many discovery cycles, moving toward scientific agents capable of extended self-improvement.
- **Breakthroughs in Algorithmic and Empirical Discovery:** InternAgent-1.5 demonstrates strong performance in both algorithm discovery and empirical scientific discovery. It produces competitive algorithmic solutions in domains such as reinforcement learning and test time methodology, and generates high quality outputs for data oriented scientific tasks. In empirical settings, the system executes complete experimental workflows and identifies new insights in fields that include biology and earth sciences. These results illustrate the generality and practical effectiveness of the framework across computational and physical scientific environments.

With these capabilities and results, we now present the design principles and technical foundations that enable InternAgent-1.5 to operate as a unified system for scientific discovery.

2. InternAgent-1.5

2.1. System Overview

In this section, we present the system overview of InternAgent-1.5 as illustrated in Fig. 3. The system automates the full research cycle by integrating hypothesis formulation, methodological evaluation, and evidence driven refinement into a unified and continuously improving process. Its operation relies on foundational capabilities that support deep research, solution refinement, and long horizon memory. These capabilities are realized through agent driven reasoning and system level infrastructure and allow the system to maintain contextual continuity across iterations. With this capability structure,

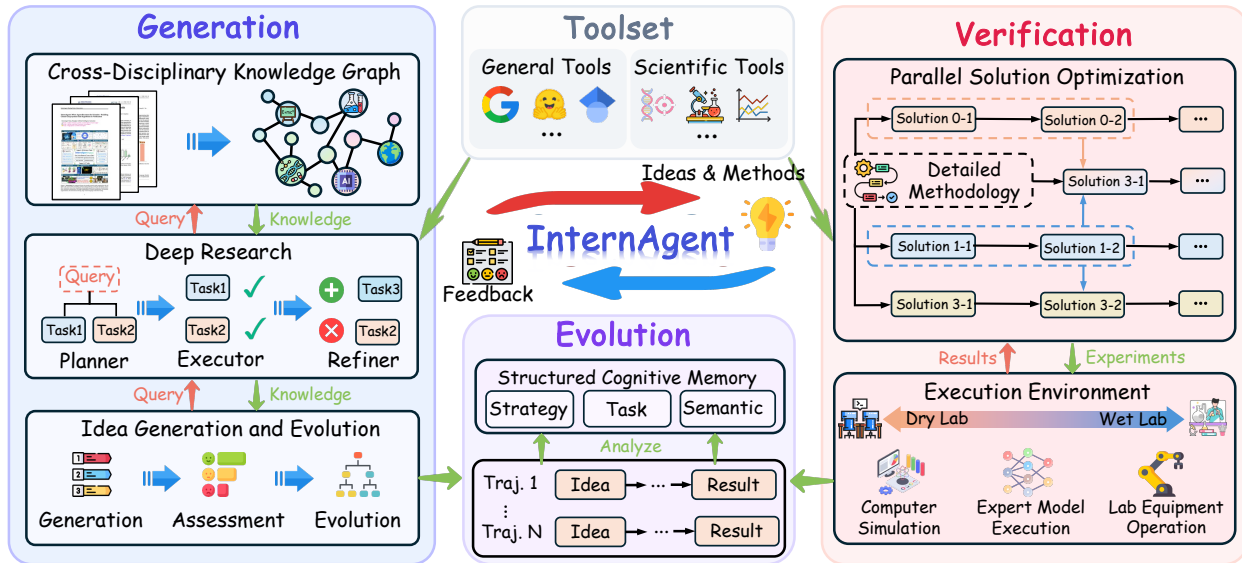


Figure 3 | Overview of InternAgent-1.5, illustrating its unified scientific discovery pipeline organized around the **Generation**, **Verification**, and **Evolution** subsystems. The system operates through foundational capabilities for deep research, solution refinement, and long horizon memory, which together enable sustained autonomous scientific discovery.

InternAgent-1.5 coordinates multiple subsystems to support autonomous, scalable, and sustained scientific discovery.

2.1.1. Architecture

The architecture of InternAgent-1.5 is organized into three core subsystems, namely the **Generation**, the **Verification**, and the **Evolution**. These subsystems form an integrated and iterative workflow. The Generation subsystem formulates hypotheses and methodological plans, the Verification subsystem evaluates these plans through computational or empirical procedures, and the Evolution subsystem incorporates the resulting evidence to update internal knowledge, strategies, and long term memory. This organization maintains a coherent flow of information and enables multi cycle autonomous operation.

- **Generation:** The Generation subsystem constructs the conceptual foundation of scientific inquiry. It follows the generation and reflection paradigm of InternAgent 1.0 [7] and is driven by the foundational capability of deep research. It conducts large scale literature analysis, scientific reasoning, and contextual integration and may invoke scientific tools when processing domain specific data. It produces structured hypotheses and methodological plans and records key reasoning traces for subsequent processing.
- **Verification:** The Verification subsystem evaluates the hypotheses and methodological plans produced by the Generation subsystem. Its operation is driven by the foundational capability of solution refinement, which structures the iterative search for improved procedures. It performs computational analyses, simulations, and laboratory style assessments as needed and uses historical information to guide evaluation choices. It supports parallel assessment of methodological variants and generates structured evidence for downstream refinement.
- **Evolution:** The Evolution subsystem refines system understanding and long term strategies based on outcomes from the Generation and Verification subsystem. It is driven by the foundational capability of memory and unifies analytical feedback with persistent knowledge management.

ment. It interprets verification results, identifies methodological limitations, updates procedural, episodic, and semantic information, and produces refined priors that guide subsequent cycles of the Generation and Verification subsystem.

These subsystems rely on the foundational capabilities introduced above in order to function coherently across extended discovery horizons. The next section presents these capabilities in detail and describes the technical methods that implement them.

2.1.2. Foundational Capabilities

The operation of InternAgent-1.5 relies on a set of foundational capabilities that allow the **Generation**, **Verification**, and **Evolution** subsystems to function coherently across extended discovery cycles. These capabilities support literature based hypothesis construction, methodological evaluation, iterative refinement, and long horizon continuity. They are implemented through the technical methods introduced in Sections 2.2 to 2.4 and provide the requirements for end-to-end scientific discovery.

The first capability is deep research. It supports the Generation subsystem by enabling large scale retrieval, integration, and structuring of cross disciplinary scientific knowledge. Section 2.2 introduces the search mechanisms and structured representations that realize this capability.

The second capability is solution refinement. It supports the Verification subsystem by guiding the refinement of methodological plans and structuring the multi round search for improved procedures. Section 2.3 presents the optimization strategies that implement this capability. Scientific tools may be invoked within this subsystem when computational or empirical assessment is required.

The third capability is long horizon memory. It supports the Evolution subsystem by maintaining persistent storage and retrieval of contextual information, reasoning traces, and experimental outcomes. Section 2.4 describes its structured organization and interaction rules.

Across these capabilities, InternAgent-1.5 maintains the continuity, adaptability, and scalability needed for reliable and continuously improving scientific discovery.

2.2. Cross Disciplinary Graph Construction and Knowledge Capturing

Deep Research Capability within the Generation Subsystem

To enable cross disciplinary knowledge construction and utilization, our design operates on both data and methodological levels. On the data side, the system integrates diverse scientific sources with the assistance of domain specific tools to parse, normalize, and structure scientific information into a large scale multidisciplinary knowledge graph. On the methodological side, it identifies relations and dependencies across domains through a structured extraction workflow that combines model driven analysis with tool assisted processing of specialized scientific data, enabling deep and effective cross disciplinary knowledge integration.

2.2.1. Cross-Disciplinary Knowledge Graph

To support accurate and comprehensive deep research, we maintain a cross-disciplinary knowledge graph (KG). Notably, it differs from traditional KGs [30, 31], which represent knowledge as triples including simple entities and relations; our KG instead captures a richer set of scientific elements.

Graph Construction From parsed outputs of papers, survey articles, technical reports, and domain notes, we construct a heterogeneous graph with nodes representing documents, key concepts, methods, datasets, empirical settings, and problem statements. The parsing process incorporates domain specific scientific tools to assist in identifying specialized entities and scientific attributes that are difficult

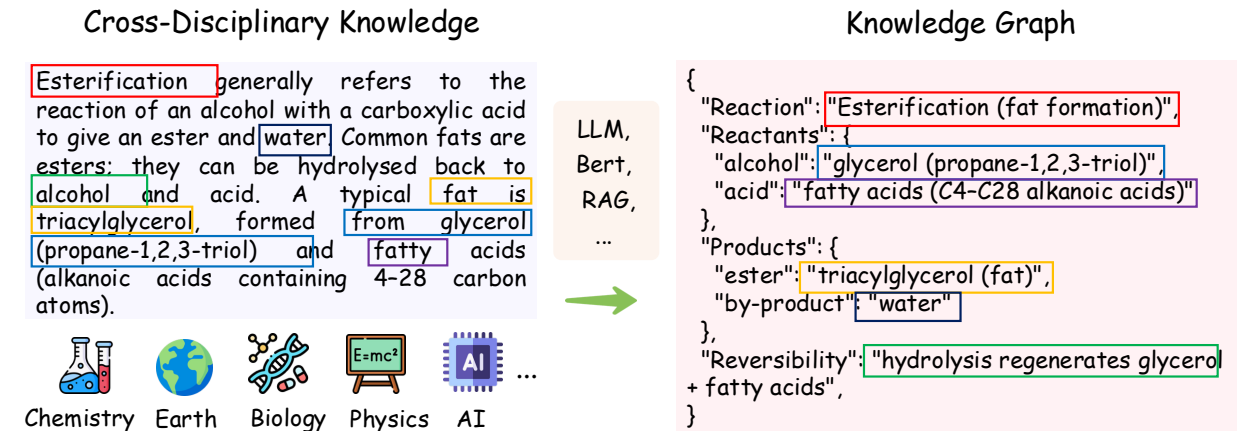


Figure 4 | The illustration for our cross-disciplinary knowledge graph.

to extract through general text analysis alone. Edges encode typed relations such as “cites” and “by product.” This design lets a single research idea sit at the intersection of multiple methodological and application communities and converts a flat corpus into a structured map where cross field dependencies emerge as paths rather than isolated points. For example, given the text “Esterification generally refers to the reaction of an alcohol with a carboxylic acid to give an ester and water. Common fats are esters; they can be hydrolysed back to alcohol and acid. A typical fat is triacylglycerol, formed from glycerol (propane 1,2,3 triol) and fatty acids (alkanoic acids containing 4–28 carbon atoms).” the corresponding structured representation is shown in Fig. 4.

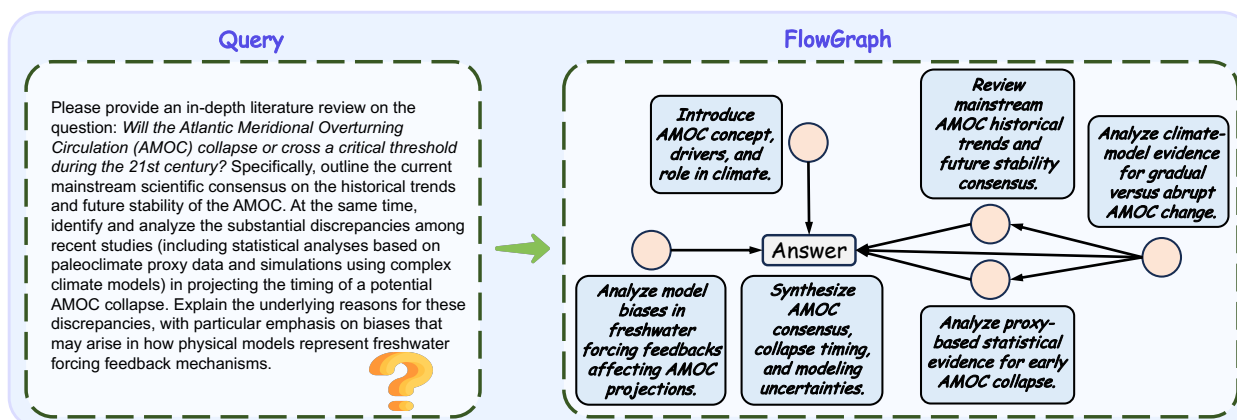


Figure 5 | The illustration for our flow graph.

Knowledge Extraction and Retrieval We employ a schema-guided extraction workflow to build a knowledge graph from noisy, cross-domain text. First, candidate entities are identified via domain-agnostic named entity recognition and noun-phrase mining, and document-level co-citation and co-usage relations are used to establish initial concept links. A subsequent consolidation step refines node types and edge semantics, aligning textual evidence with citation evidence into a compact cross-disciplinary graph. To answer deep research queries, we integrate graph search with dense vector retrieval: graph search uncovers the nodes and paths that connect the query to relevant methods and domains, while dense retrieval captures semantically related items not directly linked in the graph. Finally, a ranking step merges these results and outputs path-structured evidence chains, which the deep research module then analyzes to reveal cross-disciplinary connections.

2.2.2. Flow Graph

In real scientific deep research tasks, knowledge often exhibits highly non-linear and dynamic dependencies. Conventional sequential research process struggle to capture these relationships effectively, which can lead to redundant information, over-reliance on early hypotheses, and inflexible reasoning processes. To address these challenges, we introduce Dynamic Structured Knowledge Flow as a core principle of deep research system, enabling systematic and adaptive organization of knowledge throughout the research process. Specifically, we capture the knowledge in research process as a directed acyclic graph (DAG) that explicitly represents tasks, subtasks, and their dependencies.

Structured Knowledge Flow The research process is organized as a directed graph, which provides a structured representation of the reasoning process. Formally, the research process is defined as:

$$G = (V, E), \quad (1)$$

where V denotes the set of nodes and E denotes the set of directed edges encoding dependencies among nodes. Each node $v_i \in V$ corresponds to a subtask or a key conceptual unit arising during the reasoning process. To explicitly capture its functional role and execution status, each node is represented as a tuple:

$$v_i = (t_i, d_i, s_i, c_i), \quad (2)$$

where $t_i \in \{\text{search, solve, answer}\}$ specifies the task type associated with the node, d_i describes the task content, s_i tracks the execution state of the node, and c_i stores the resulting knowledge context upon successful completion of the task. Directed edges in the graph encode structural dependencies or reasoning constraints between nodes. Specifically, each edge is defined as:

$$e_{ij} = (v_i, v_j, r_{ij}) \in E, \quad (3)$$

where e_{ij} indicates a directed relationship from node v_i to node v_j , and r_{ij} characterizes the type of dependency between the two nodes, such as *requires result from*, *provides evidence for*, or *constrains reasoning of*. These relational edges ensure that information and intermediate results are propagated in a dependency-aware manner throughout the reasoning graph.

Dynamic planning and refinement The knowledge flow is constructed incrementally: starting from a root query node, a planner identifies nodes that require further decomposition or context enrichment, generates successor nodes, and updates dependency edges accordingly. This iterative expansion continues until the flow sufficiently covers all subproblems necessary to address the research objective. This design not only enables efficient multi-agent collaboration but also supports adaptive refinement of the knowledge flow as new evidence emerges, ensuring coherent, systematic, and verifiable reasoning throughout the research process.

2.2.3. Graph-Guided Output Synthesis

Building upon the dynamically constructed knowledge flow, we describes how the abstract graph structure is instantiated into concrete research outputs. Once the planner completes the incremental construction of the flow graph, executable nodes are activated according to their dependency states and progressively populated with domain knowledge and intermediate reasoning results. Through iterative node execution, state updating, and context propagation along graph edges, the system refines the structured knowledge flow and synthesizes the final research answer.

Cross-Disciplinary Knowledge Collector. To facilitate cross disciplinary insight, the Knowledge Collector gathers information from a diverse set of sources across multiple domains. These sources include outputs obtained through scientific tools and remote resources accessed via the Science Context Protocol (SCP) [32]. By integrating multi domain knowledge, the system can uncover unexpected connections and inspire ideas that may not emerge within a single discipline. Executable nodes with satisfied dependencies are assigned to agents, which decompose each subtask into a sequential reasoning and information retrieval process, iteratively assembling the knowledge required to resolve it. After a node is executed, its state is updated and the resulting knowledge context is propagated to dependent nodes, ensuring that subsequent reasoning benefits from the most up to date and contextually rich information. This design enables structured, adaptive, and collaborative knowledge acquisition throughout the research process.

Reasoning capability enhancement We adopt a reasoning capability enhancement strategy that enables reasoning along multiple complementary pathways. For a given query, the model generates three forms of responses: a direct answer based solely on the input, a search augmented answer that incorporates evidence retrieved from external sources and scientific tools, and a self driven answer obtained through internal retrieval and refinement. These complementary outputs are aggregated to form the final response, balancing intrinsic reasoning, external evidence, and self consistency. This multi path strategy improves answer completeness and factual reliability while reducing reliance on any single reasoning pathway.

2.3. Experiment Execution and Multi-round Parallel Optimization

Solution Refinement Capability within the Verification Subsystem

The transformation of a refined methodology into a verifiable scientific result requires an efficient and reliable validation loop. In both computational algorithm design and physical wet-lab experimentation, the search space of possible configurations is extremely large, and linear trial-and-error procedures often converge prematurely. This section introduces the multi-round parallel experiment optimization and execution framework, which enables InternAgent-1.5 to explore this space autonomously and progressively converge toward high-quality experimental proposals.

2.3.1. Generative Design for Experimental Optimization

Efficiently exploring a large and unstructured design space is a central challenge in automated scientific experimentation. Traditional strategies [33, 34] based on linear refinement or tree-structured search often face three fundamental limitations: **Isolated Trajectories** arise when insights discovered in one search path cannot inform parallel explorations. **Unexploited Search History** occurs when informative patterns across longer trajectories are not captured or reused. **Limited Idea Composition** restricts the integration of promising elements from different branches into improved solutions.

We formalize the experimental optimization problem as identifying the optimal solution within a search space \mathcal{S} , where each candidate solution $s \in \mathcal{S}$ represents a complete experimental proposal, including code logic, parameter configurations, and physical operation protocols. The objective is to find:

$$s^* = \arg \max_{s \in \mathcal{S}} h(\mathcal{T}, s), \quad (4)$$

where $h(\mathcal{T}, s)$ denotes the evaluation metric of solution s on a given task \mathcal{T} .

To address the limitations of conventional search, InternAgent-1.5 adopts a *Graph-Augmented Monte Carlo Search* framework. This approach preserves the exploration–exploitation balance of Monte Carlo Tree Search while replacing its rigid tree structure with a dynamic solution graph that aggregates

information across all prior experiments. The search still follows the classical loop of selection, expansion, simulation, and backpropagation, but its effectiveness comes from a strengthened expansion phase powered by four graph-based operators:

- **Primary Expansion.** Generates a new proposal using only its immediate parent. It performs localized adjustments such as parameter refinement or correction of logical inconsistencies, creating the core backbone of parent and child edges used in credit assignment.
- **Intra-branch Evolution.** Conditions proposal generation on both the parent and the historical trajectory of ancestors within the same branch. By analyzing recent successes and failures, it reinforces productive design changes and avoids repeatedly exploring unpromising strategies, formalizing a localized form of self-reflection.
- **Cross-branch Reference.** Introduces targeted transfer of design elements across different branches. When a branch stagnates, the system identifies high-performing nodes elsewhere in the solution graph and uses them as references, allowing the new proposal to incorporate robust structural patterns or methodological modules discovered in parallel explorations.
- **Multi-branch Aggregation.** Synthesizes complementary strengths from multiple top-performing nodes across the solution graph. By decomposing these proposals into their essential components and recombining them, the operator produces hybrid designs that integrate successful ideas from previously independent search trajectories.

Once a new proposal is generated through one of these operators, it is executed in the corresponding environment, either a computational simulator or a physical experimental system, to obtain an evaluation score. This score is backpropagated through the proposal's ancestral path to guide subsequent exploration. By integrating graph-based information flow into the Monte Carlo search process, InternAgent-1.5 transforms experimental design into a collaborative and cumulative optimization pipeline, enabling rapid convergence toward high-quality scientific solutions.

2.3.2. Scenario

Code Optimization for Algorithm Discovery In algorithm discovery tasks, each proposal is an executable program specifying data-processing steps, model components, and evaluation settings. The search module generates new variants by refining computational logic or integrating effective structures identified in other branches. Each candidate is executed in a controlled environment that compiles the code and evaluates its performance on benchmark datasets. Quantitative metrics such as accuracy, runtime, and resource usage are returned to the optimization module and backpropagated through the proposal's lineage, enabling systematic refinement of algorithmic designs.

Experimental Optimization for Empirical Discovery In empirical discovery tasks, each proposal specifies a full experimental procedure that may be executed either through computational simulation or on physical laboratory systems. The search process refines these procedures by adjusting parameters, modifying operational steps, or incorporating effective sub-protocols identified across branches. When a proposal is simulated, domain models predict experimental outcomes such as reaction yield or protein stability. When it is executed physically, SCP [32] coordinates automated devices to perform the protocol and collect measurements such as fluorescence intensity or assay signal quality. All quantitative results, whether simulated or physically measured, are returned to the optimization module for backpropagation, enabling iterative improvement of empirical workflows.

2.4. Structured Cognitive Memory for Long Horizon Scientific Discovery

Long Horizon Memory Capability within the Evolution Subsystem

To support adaptive, efficient, and long horizon scientific discovery, InternAgent-1.5 incorporates a hierarchical memory subsystem referred to as Structured Cognitive Memory. This subsystem is

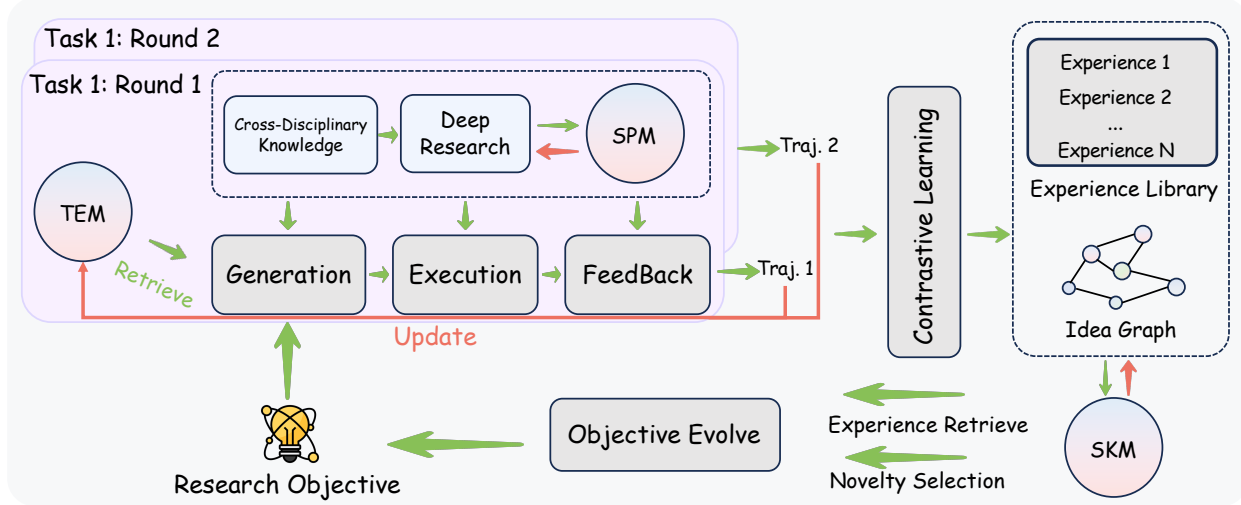


Figure 6 | The illustration for our Structured Cognitive Memory.

engaged throughout the entire discovery loop and maintains continuity across cycles, allowing the agent to operate coherently over extended durations. It consolidates procedural, episodic, and semantic information into a unified structure that enables short term refinement, mid term adaptation, and long term conceptual development. The overall framework of Structured Cognitive Memory is shown in Fig. 6.

2.4.1. Strategy-Procedural Memory

Strategy Procedural Memory (SPM) supports the deep research capability that InternAgent-1.5 invokes throughout the entire scientific discovery process whenever complex analytical reasoning is required. This capability involves integrating literature evidence, synthesizing contextual knowledge, constructing coherent multi-step reasoning plans, correcting failed strategies from earlier research workflows, and analyzing the root causes behind those failures. Instead of storing raw trajectories, the system distills reusable procedural structures from past reasoning processes, including both validated effective patterns and lessons learned from unsuccessful attempts. These procedural structures capture the key decision pivots, organizational patterns that have proven effective across earlier research workflows, as well as the diagnostic insights into failed strategies and their underlying reasons, serving as strategic priors that can be applied flexibly at different stages of the pipeline to avoid recurring pitfalls and optimize reasoning paths.

Given a historical trajectory T , SPM constructs a compact representation as follows:

$$\mathbf{z}_T = f_{\text{proc}}(T), \quad (5)$$

which captures essential procedural states extracted from the full execution trace. When a new deep research query q arrives, InternAgent-1.5 retrieves trajectories with procedurally aligned structures:

$$S(q) = \underset{T \in \mathcal{M}_{\text{SPM}}}{\text{topk}} \sim(f_{\text{proc}}(q), \mathbf{z}_T). \quad (6)$$

These retrieved strategic priors guide the planner toward globally coherent reasoning graphs, while constraining the executor to avoid redundant execution steps and unnecessary tool calls, thereby providing a stable and efficient procedural foundation for the downstream discovery process.

2.4.2. Task-Episodic Memory

Task Episodic Memory (TEM) supplies fine grained, within trajectory evidence that enables rapid adaptation during iterative experimentation. After each experiment, the system stores an episodic unit containing the attempted method m , extracted metrics y , and an improvement judgment. Each unit is encoded using a hybrid representation that combines semantic embeddings with sparse lexical features to support both conceptual and literal alignment.

During hypothesis refinement, relevant episodes are retrieved through the following formula:

$$\mathcal{R}(q) = \underset{e \in \mathcal{E}}{\text{topk sim}}(f_{\text{enc}}(q), f_{\text{enc}}(e)), \quad (7)$$

where q denotes the current hypothesis. The retrieved episodes are injected directly into the generation context, helping the system avoid unsuccessful methodological directions, exploit successful ones, and refine hypotheses efficiently within each research trajectory.

2.4.3. Semantic-Knowledge Memory

Semantic Knowledge Memory (SKM) consolidates conceptual information across sessions and supports the long horizon evolution of research objectives. It consists of a Long Term Experience Library, which stores distilled methodological insights, and an Idea Graph that tracks the semantic topology of previously explored research directions. Specifically, upon the end of each experimental batch, the system employs a pairwise combination strategy for the generated methods to maximize the utilization of existing information. By leveraging contrastive learning between each combination according to their methods and experimental results, InternAgent-1.5 extracts both high-level methodological principles and low-level experimental heuristics to construct Long-term Experience Library. Given a research goal G , long term knowledge entries are retrieved via the following formula:

$$\mathcal{K}(G) = \underset{k \in \mathcal{L}}{\text{topk sim}}(f_{\text{enc}}(G), f_{\text{enc}}(k)). \quad (8)$$

To promote continued exploration, each candidate objective c is assigned a novelty score:

$$\text{nov}(c) = 1 - \underset{x \in \mathcal{G}}{\text{max sim}}(f_{\text{enc}}(c), f_{\text{enc}}(x)), \quad (9)$$

which encourages the selection of objectives that extend beyond previously explored conceptual regions. In this way, SKM provides the semantic continuity and innovation pressure required for sustained multi-session scientific discovery.

3. Experiments

To evaluate InternAgent-1.5’s capabilities in the full process of scientific discovery from multiple aspects, we verify its effectiveness through cross-disciplinary benchmarks, autonomous algorithm development, and scientific mechanism discovery, as elaborated in Sec. 3.2, 3.3, and 3.4, respectively. In Sec. 3.4, InternAgent-1.5 demonstrates its applications in scenarios such as Earth Science 3.4.1, Life Science 3.4.2, Biological Science 3.4.3, and Physical Science Tasks 3.4.4.

3.1. Experiments Setup

3.1.1. General Scientific Reasoning Abilities

SGI-Bench [29]. SGI-Bench is a scientist-aligned benchmark for Scientific General Intelligence (SGI), defined as the ability of an AI system to autonomously navigate the full scientific inquiry cycle of

Deliberation, Conception, Action, and Perception. It operationalizes this goal with four task families spanning 10 scientific disciplines and 1,000+ expert-curated samples: Scientific Deep Research, Idea Generation, Dry/Wet Experiments, and Experimental Reasoning. Our results are reported on the DeepResearch and IdeaGeneration subsets.

GAIA [25]. GAIA is a benchmark of real-world tasks that require coordinated abilities in reasoning, multimodal understanding, web navigation, and tool use. We report results on its 165-question validation set.

HLE [27]. Humanity’s Last Exam (HLE) is a large-scale multimodal benchmark of 2,500 expert-written questions covering mathematics, humanities, and the natural sciences. It is designed to probe frontier-level academic reasoning, where current LLMs still fall far short of human performance.

Frontier Science [28]. FrontierScience is a benchmark that evaluates whether AI systems can perform expert-level scientific tasks, including study design, data interpretation, and hypothesis assessment. Following the protocol in the original paper, our results are averaged over 20 runs on the Olympiad subset and 30 runs on the Research subset using its standard evaluation set.

GPQA-diamond [26]. GPQA is a collection of 448 expert-written multiple-choice questions in biology, chemistry, and physics, designed to test deep scientific reasoning rather than surface knowledge. We use its 198-question GPQA-diamond subset for evaluation.

3.1.2. Algorithm Discovery

Scientific Algorithm. To validate the ability of InternAgent-1.5 to discover algorithms in scientific data domains and to demonstrate its improvements over InternAgent-1.0 [7], we conducted experiments on six scientific data oriented algorithm discovery tasks. Notably, due to the limited capabilities of the coding agent in InternAgent-1.0 [7], the baseline repositories for all tasks were first manually consolidated into single-file implementations before being optimized by our system. In contrast, *InternAgent-1.5 supports an end-to-end algorithm optimization workflow directly on the original codebases*.

- **AutoRYP:** The AutoRYP task is built on the Suzuki–Miyaura reaction dataset containing 5,760 reaction entries [35]. A LoRA-finetuned LLaMA3-8B embedding model [36] with an MLP predictor serves as the baseline. Model performance is assessed using the coefficient of determination (R^2).
- **AutoTPPR:** The AutoTPPR task operates on the Perturb-seq single-cell transcription-response dataset [37]. GEARS [38], a GNN- and MLP-based framework for multi-omics representation learning, is adopted as the baseline. The Top-20 DE MSE is used as the evaluation metric.
- **AutoPower:** The AutoPower task relies on the IEEE 39-Bus benchmark for power-flow estimation [39]. SenseFlow [40], a physics-informed self-ensembling model, serves as the baseline method. Evaluation is performed using RMSE on PQ nodes.
- **AutoTSF:** The AutoTSF task is defined on the ETTh1 multivariate time-series dataset from the ETT benchmark [41]. DLinear [42], an MLP-based decomposition and forecasting model, is used as the baseline. Mean Absolute Error (MAE) averaged over horizons 96, 192, 336, 720 serves as the metric.
- **AutoMD:** The AutoMD task uses the MD17 dataset [43], which provides molecular energies and forces for seven small organic molecules. VisNet [44], an equivariant geometry-enhanced GNN, is adopted as the baseline. Force-MAE is used as the evaluation metric.
- **AutoEAP:** The AutoEAP task is constructed from the UMI-STARR-seq enhancer-activity dataset [45]. DeepSTARR [46] provides the baseline for sequence-based enhancer-activity prediction. Housekeeper Pearson Correlation Coefficient (HK-PCC) is used for evaluation.

AI Algorithm. To further evaluate the capabilities of InternAgent-1.5 on AI algorithm discovery, we assembled a diverse suite of tasks that span model training pipelines, memory optimization strategies, reinforcement learning methods, and data processing routines, which collectively represent several of the most active directions in current AI algorithm research. *For each domain, we selected papers accepted by top AI conferences in 2025 as comparative baselines to validate whether InternAgent-1.5 can outperform the latest AI algorithms.*

- **AutoTTS:** The AutoTTS task is constructed on a benchmark evaluating test-time scaling strategies for enhancing LLM reasoning. Atom [47], a Markov-structured test-time scaling framework that refines reasoning through iterative candidate exploration and denoising, serves as the baseline. Model performance is assessed using standard accuracy-based reasoning metrics defined by the benchmark.
- **AutoMem:** The AutoMem task is defined on long-term interaction and memory-management benchmarks for LLM agents. A-MEM [48], an agentic memory system inspired by the Zettelkasten method and designed for dynamic note construction, semantic linking, and memory evolution, serves as the baseline. Evaluation focuses on long-horizon agent performance using metrics such as retrieval accuracy, contextual relevance, and behavioral consistency under extended interaction.
- **AutoLM:** The AutoLM task examines self-distillation based data synthesis for mathematical reasoning. For comparison, we implement a complete self-distillation pipeline that performs synthetic question creation through few-shot prompting, reasoning-trajectory generation, and answer verification through majority voting. The resulting synthetic data are then used to train Intern-S1-mini [49]. The evaluation measures the mathematical-reasoning ability of the resulting model, using standard question-answering accuracy as the primary metric.
- **AutoTTRL:** The AutoTTRL task is designed to autonomously discover reinforcement learning algorithms that do not require ground truth annotations on reasoning tasks (*i.e.*, AIME 2024 [50]). We employ Test-Time Reinforcement Learning (TTRL) [51] as the baseline method, which utilizes a majority voting mechanism to provide effective reward estimation. Following TTRL, we generate 16 responses per question and calculate the average pass rate $\text{pass}@1 = \frac{1}{k} \sum_{i=1}^k p_i$ for evaluation, where p_i denotes the correctness of the i -th response.

3.1.3. Empirical Discovery

Earth Science. To evaluate InternAgent-1.5 in the Earth Science domain, which involves petabyte-scale, multi-dimensional datasets and complex physical processes, we constructed two representative tasks:

- **Automated Climate Diagnostics:** This task assesses the system's ability to integrate multi-source knowledge for data analysis. The benchmark utilizes historical Surface Air Temperature (TAS) data (1970–2010) from 20 Global Climate Models (GCMs) in the CMIP6 archive [52] (including ACCESS-ESM1-5, CanESM5, etc.) and the ERA5 reanalysis dataset [53] as the observational ground truth. The goal is to autonomously identify global warming trends and regional biases.
- **Climate Downscaling Optimization:** This task evaluates the system's ability to innovate scientific methods. The objective is to enhance surface-temperature fields over China from coarse-resolution NCEP-NCAR-R1 data (2°) [54] to fine-scale ERA5 resolution (0.25°). We employ standard Kriging interpolation [55] and linear Bias-Corrected Spatial Disaggregation (BCSD) [56] as baselines to test if the system can autonomously design a superior deep-learning-based solution.

Life Science. To demonstrate the broad applicability of InternAgent-1.5 in early-stage drug discovery, we evaluate its capabilities to therapeutic target identification, a domain characterized by heterogeneous multi-omics evidence, complex disease mechanisms, and strong requirements for mechanistic interpretability and experimental verifiability. We construct two representative target-discovery tasks that stress graph-structured planning, multi-modal tool orchestration, and iterative reflection:

- **Automated Biological Evidence Synthesis:** The agent orchestrates end-to-end analyzes (expression, genomic alteration, survival, pathway, and tractability) by integrating resources such as TCGA [57], OpenTargets [58] and KEGG [59], and synthesizes a coherent evidence chain. We reproduce OriGene’s discovery of *GPR160* as an HCC target.
- **Hypothesis Generation and Target Prioritization:** The agent constructs a multi-modal evidence graph (cohorts, proteomics, annotations, pathways, and literature) and iteratively refines mechanistic hypotheses to rank actionable candidates. We reproduce the identification of *ARG2* as a mechanistically grounded target in CRC, together with experiment-ready validation suggestions.

Biological Sciences. As a key capability in the Biological Sciences domain, the fluorescent-protein engineering task targets the improvement of existing fluorescent proteins for imaging applications. The system identifies the parent sequence and relevant structural context through literature-driven analysis, then performs dry-lab design by combining sequence inspection, folding prediction with ESMFold [60], and mutational-effect evaluation using sequence–function and stability predictors such as ProSST [61] to generate candidate variants. These designs are translated into wet-lab protocols through SCP [32], which coordinates automated DNA assembly, expression, purification, and fluorescence-intensity measurement. The resulting data are analyzed and fed back into the design layer, producing a structured experimental report that integrates predictions, protocols, and measured performance.

Physical Science. To evaluate InternAgent-1.5 in chemical synthesis and drug discovery, we define two tasks requiring the integration of physical constraints and structural design:

- **Automated Reaction Outcome Prediction:** Evaluated on the ChemCoTBench [62] forward prediction dataset, this task requires the agent to predict both the target major product and stoichiometric by-products. The system must analyze reactant properties and strictly apply atomic conservation logic. To ensure rigorous evaluation, we explicitly revised 26 problematic entries in this benchmark, providing a corrected ground truth for synthesis planning.
- **Generative Scaffold Hopping:** This task aims to discover novel molecular entities that circumvent patent barriers while preserving bioactivity. The agent is tasked with replacing the core scaffold of a molecule while maintaining key 3D shape and electrostatic features. The system must employ generative algorithms to propose bioisosteres and filter candidates based on medicinal chemistry metrics, such as Synthetic Accessibility and LogP, to ensure the proposed analogs are viable drug candidates.

3.2. Evaluating Agentic Reasoning Abilities

SGI-Bench. As shown in Table 2, InternAgent-1.5 (Gemini-3-pro+o4-mini) achieves the best performance on two SGI-Bench tracks, Deep Research and Idea Generation, significantly outperforming strong frontier models. On Deep Research track, InternAgent-1.5 reaches 37.74%, surpassing the second-best Gemini-3-pro 18.48% by a large margin (+19.26%). On Idea Generation, InternAgent-1.5 attains 58.11%, exceeding the prior best GPT-5 55.40% (+2.71%). Overall, these results suggest that InternAgent-1.5’s iterative deep-research workflow that integrate structured planning, targeted

Table 2 | Performance comparison on SGI-bench. The best results are **bolded** and the second best results are underlined.

Method	Deep Research	Idea Generation
Gemini-3-pro [63]	<u>18.48</u>	39.68
GPT-5 [64]	14.47	<u>55.40</u>
Claude-Sonnet-4.5 [65]	13.84	43.20
Qwen3-Max [66]	15.38	39.83
o4-mini [67]	11.95	40.78
InternAgent-1.5 (Gemini-3-pro+o4-mini)	37.74	58.11

Table 3 | Performance comparison on GAIA and HLE benchmarks. The best results are **bolded** and the second best results are underlined. Results not reported in the original papers are denoted as “ - ”.

Agent	Base Model	GAIA val				HLE	
		Level 1	Level 2	Level 3	Avg.	Text only	All
<i>React Model with Tools</i>							
WebDancer [68]	QwQ-32B	61.5	50.0	25.0	51.5	-	-
WebShaper [69]	Qwen2.5-72B	69.2	63.4	16.6	60.1	-	-
MiroThinker [70]	MiroThinker-v1.5-30B	-	-	-	72.0	31.0	
MiroThinker [70]	MiroThinker-v1.5-235B	-	-	-	80.8	<u>39.2</u>	-
Tongyi-DR [71]	Tongyi-DR-30B	-	-	-	70.9	32.9	-
<i>DeepResearch Agents</i>							
OpenAI DR [72]	-	74.29	69.06	47.60	67.36	-	26.60
ChatGPT-Agent [64]	-	-	-	-	-	-	41.60
Kimi-Researcher [73]	-	-	-	-	-	-	26.90
Manus [74]	-	<u>86.50</u>	<u>70.10</u>	<u>57.70</u>	73.30	-	-
Gemini DR [75]	-	-	-	-	-	-	26.90
OWL [76]	Gemini 2.5 Pro	84.90	68.60	42.30	69.70	-	-
<i>Our Method</i>							
InternAgent-1.5	Qwen3-235B	69.81	60.47	30.77	58.79	15.04	14.84
InternAgent-1.5	o4-mini	88.68	81.39	61.54	80.61	36.10	34.52
InternAgent-1.5	Gemini-3-pro+o4-mini	92.45	89.53	61.54	86.06	40.87	40.00

information gathering, and refinement yields substantial gains in evidence-driven research capability while also improving creative yet grounded idea generation.

GAIA. As shown in Table 3, InternAgent-1.5 outperforms both closed-source Manus (73.30%) and leading open-source agentic models Mirothinker (80.8%) and Tongyi-DR (70.9%), even though they are specifically trained and evaluated only on the GAIA text-only subset. InternAgent-1.5 also shows strong robustness on Level 3 questions (61.54%). These results indicate that InternAgent-1.5’s iterative workflow combining knowledge planning, collection, and refinement is particularly effective for multi-hop and compositional reasoning.

HLE. As shown in Table 3 and 4, InternAgent-1.5 achieves the best overall performance among all compared systems. It reaches 40.87% accuracy in the text-only setting and 40.00% on the full benchmark, outperforming strong baselines such as Gemini-3-pro-preview and GPT-5. The

Table 4 | Domain-wise performance comparison on the Humanity’s Last Exam (HLE). The best results are **bolded** and the second best results are underlined.

		Humanity’s Last Exam								
Setting	Model	Math	Bio/Med	CS/AI	Physics	Human.	Chem.	Engineer.	Other	Avg.
Text-Only	Deepseek-R1 [77]	9.30	8.60	7.40	5.80	11.00	5.60	10.30	7.50	8.60
	Gemini-3-pro-preview [63]	<u>45.08</u>	<u>26.13</u>	<u>26.79</u>	<u>32.67</u>	<u>44.04</u>	<u>34.65</u>	<u>29.69</u>	<u>32.39</u>	<u>38.00</u>
	InternAgent-1.5	48.96	30.63	29.46	34.16	44.56	<u>30.69</u>	<u>28.13</u>	<u>37.50</u>	40.87
All-Set	o4-mini [67]	19.00	11.40	12.90	12.60	9.10	12.70	12.60	6.90	14.30
	GPT-5 [64]	31.00	22.10	24.90	21.70	20.60	16.40	14.40	18.00	24.80
	Gemini-3-pro-preview [63]	<u>44.76</u>	<u>27.14</u>	<u>29.05</u>	<u>31.30</u>	42.92	40.00	32.43	<u>34.33</u>	<u>38.04</u>
	InternAgent-1.5	48.09	30.36	30.71	33.04	<u>42.47</u>	<u>34.55</u>	<u>30.63</u>	38.63	40.00

Table 5 | Performance comparison on FrontierScience of olympiad and research tasks across bio, chem, and phy domains. The best results are **bolded** and the second best results are underlined.

Method	Olympiad (avg N=20)				Research (avg N=30)			
	Bio	Chem	Phy	All	Bio	Chem	Phy	All
o4-mini [67]	47.00±14.90	65.00±6.40	53.40±4.50	57.40±3.30	9.67±5.47	8.17±4.37	0.83±2.27	6.20±2.54
InternS1-235B [78]	17.00±12.69	52.88±4.05	50.40±3.88	48.05±2.84	4.50±4.35	11.00±3.74	2.67±3.35	6.06±2.30
Mirothinker-v1.5-30B-A3B [70]	22.86±4.52	69.64±7.49	54.86±3.18	57.57±3.66	8.17±6.39	8.50±6.21	5.83±4.10	7.50±3.77
DeepSeek-V3.2-Thinking [79]	26.50±7.26	72.25±3.25	66.30±2.63	64.70±2.41	2.50±3.10	16.33±4.64	1.40±2.70	6.84±1.88
Qwen3-235B-A22B-Thinking [66]	24.00±9.17	61.13±6.05	57.10±4.79	55.40±3.68	10.17±5.08	10.00±6.32	1.58±2.41	7.34±3.37
Qwen3-30B-A3B-Thinking [66]	13.50±9.10	47.25±4.47	42.70±3.65	41.60±2.94	1.50±2.93	2.00±3.32	0.70±1.79	1.41±1.52
<i>Our Method</i>								
InternAgent-1.5	46.00±8.00	85.50±3.67	76.80±2.99	77.20±3.06	10.33±4.64	22.00±6.00	3.67±2.87	12.00±2.49

improvements are consistent across most HLE sub-domains, highlighting the robustness of InternAgent-1.5 on long-horizon, cross-disciplinary reasoning tasks.

FrontierScience. Table 5 compares the performance of various methods on Olympiad and Research tasks across biology, chemistry, and physics domains. InternAgent-1.5 achieves the best overall results in both Olympiad (77.20%) and Research (12.00%) settings, with particularly strong performance in Chemistry and Physics. It outperforms all baselines, including DeepSeek-V3.2-Thinking (64.70% Olympiad) and Mirothinker-v1.5 (7.50% Research), demonstrating its superiority in both structured problem-solving and open-ended scientific reasoning.

GPQA. As shown in Table 6, InternAgent-1.5 achieves state-of-the-art performance on the GPQA-diamond benchmark with an average accuracy of 87.37%. It outperforms both strong base models and prior tool-augmented agents, with particularly strong results in Chemistry and Physics. These results demonstrate the effectiveness of our method for expert-level scientific reasoning.

3.3. Results for Algorithm Discovery Tasks

3.3.1. Scientific Algorithm

We evaluated InternAgent-1.5 across six scientific domains and compared it against our previous work [7, 21], and state-of-the-art domain-specific baselines. As summarized in Table 7, InternAgent-1.5 consistently achieves superior performance across all tasks and demonstrates the efficacy of our architectural improvements.

Chemical and Molecular Analysis. In the domain of chemical synthesis, the model demonstrates a strong capacity to interpret structured reaction information. For the AutoRYP task on the Suzuki-Miayura dataset, InternAgent-1.5 achieves an R^2 of 36.6. This result significantly outperforms the LoRA finetuned LLaMA3 baseline of 27.6 and the Dolphin score of 31.8. Similarly, for the AutoMD

Table 6 | Performance comparison on GPQA-diamond benchmark. The best results are **bolded** and the second best results are underlined. Results not reported in the original papers are denoted as “ - ”.

Agent	GPQA-diamond			
	Bio	Chem	Phys	Avg.
Base Models				
Qwen-3-8B [66]	-	-	-	44.44
Qwen3-32B [66]	-	-	-	49.49
Qwen3-235B [66]	-	-	-	47.47
Intern-S1 [78]	89.47	59.49	93.02	78.26
Deepseek-R1 [77]	63.16	<u>76.34</u>	91.86	82.32
o4-mini [67]	78.95	<u>63.44</u>	94.19	78.28
GPT-5 [64]	84.21	<u>76.34</u>	<u>95.35</u>	<u>85.35</u>
React Model with Tools				
WebShaper [69]	47.37	52.69	81.40	64.65
MiroThinker [80]	<u>84.21</u>	75.27	<u>95.35</u>	84.85
Tongyi DR [71]	78.95	67.74	<u>95.35</u>	80.30
Our Method				
InternAgent-1.5	<u>84.21</u>	79.57	96.51	87.37

Table 7 | Performance comparison across six types of scientific algorithm tasks.

Method	Tasks					
	AutoRYP	AutoTPPR	AutoPower	AutoTSF	AutoMD	AutoEAP
	R^2	MSE	RMSE	MAE	Energy-MAE	HK-PCC
Baseline	27.6	0.197	0.00473	0.438	0.158	0.65
Dolphin [21]	31.8	0.173	0.00455	0.463	0.152	0.76
InternAgent-1.0 [7]	35.4	0.146	0.00426	0.433	0.148	0.79
InternAgent-1.5	36.6	0.143	0.00318	0.423	0.114	0.91

task regarding Molecular Dynamics, our model effectively captures geometric features. It reduces the Energy MAE to 0.114 compared to 0.158 achieved by the equivariant GNN baseline VisNet.

Physics and Engineering Systems. Our framework exhibits robust performance in modeling complex physical systems and temporal dependencies. In the AutoPower task for Power Flow Estimation, InternAgent-1.5 achieves an RMSE of 0.00318 on the IEEE 39-Bus dataset. This surpasses the physics informed SenseFlow model score of 0.00473. For the AutoTSF task involving Time Series Forecasting, the DLinear baseline proves to be a strong competitor with an MAE of 0.4382. Our method further reduces the error to 0.423 and demonstrates effective handling of multivariate trends in the ETTh1 dataset.

Biological and Genomic Prediction. The most substantial improvements are observed in computational biology tasks. In the AutoTPPR task for Transcription Prediction, the model achieves an MSE of 0.143. This outperforms the GNN based GEARS framework score of 0.197. Notably, in the AutoEAP task for Enhancer Activity Prediction, InternAgent-1.5 reaches a Pearson Correlation Coefficient of 0.91. This constitutes a drastic improvement over the DeepSTARR baseline of 0.65 and highlights the exceptional ability of the agent to map DNA sequences to quantitative activity levels.

Table 8 | Results on complicated scientific algorithm design tasks. Note that our previous version Dolphin [21] and InternAgent-1.0 [7] cannot address these complicated tasks listed in the table.

Method	Tasks			
	AutoTTS	AutoMem	AutoTTRL	AutoLM
	Acc	F1	Acc	Acc
Baseline	70.9	0.2338 ± 0.3452	23.3	0.880
InternAgent 1.5	72.5	0.2785 ± 0.3643	23.9	0.904

3.3.2. AI Algorithm

Test-time Scaling. On the MMLU-CF dataset [81], we evaluate the reasoning capability using the architecture proposed by [47]. Our approach attains a score of 72.5, exceeding the baseline score of 70.9. This improvement indicates that InternAgent-1.5 effectively enhances performance in knowledge-intensive tasks, demonstrating robust reasoning capabilities and superior adaptability in complex domain scenarios.

Memory Mechanism. On the Locomo dataset [82], we evaluate under the AutoMem setup using Qwen2.5-3B [66] as the base model to ensure alignment with the A-MEM [48] baseline. Using F1 as the evaluation metric, our approach attains an F1 of 0.2785, exceeding the baseline score of 0.2338. This improvement indicates that the proposed memory architecture and interaction mechanism enable more reliable long-horizon retention, retrieval, and integration of accumulated information.

Reinforcement Learning. On the AutoRL task, we evaluate our approach across the reinforcement-learning control and decision-making benchmarks used in prior work. Using the same environments and return-based metrics as the TTRL baseline, our method achieves consistently higher returns and improved training stability. These results indicate that the proposed framework provides more effective trajectory refinement and decision-making guidance across diverse RL settings.

Large Language Model. On the AutoLM task, we apply the full self distillation pipeline and fine tune Intern-S1-mini [78] on the synthesized mathematical reasoning data. To validate algorithmic performance under a minimal system configuration, all experiments are conducted with a 16k token context. We evaluate our approach on the MATH500 reasoning benchmark used in prior work. Accuracy improves from 0.880 to 0.904, indicating that the enhanced self distillation pipeline produces higher quality trajectories and verified answers, providing effective supervision for strengthening the model’s mathematical reasoning ability.

3.4. Discoveries of Scientific Mechanism

3.4.1. Earth Science

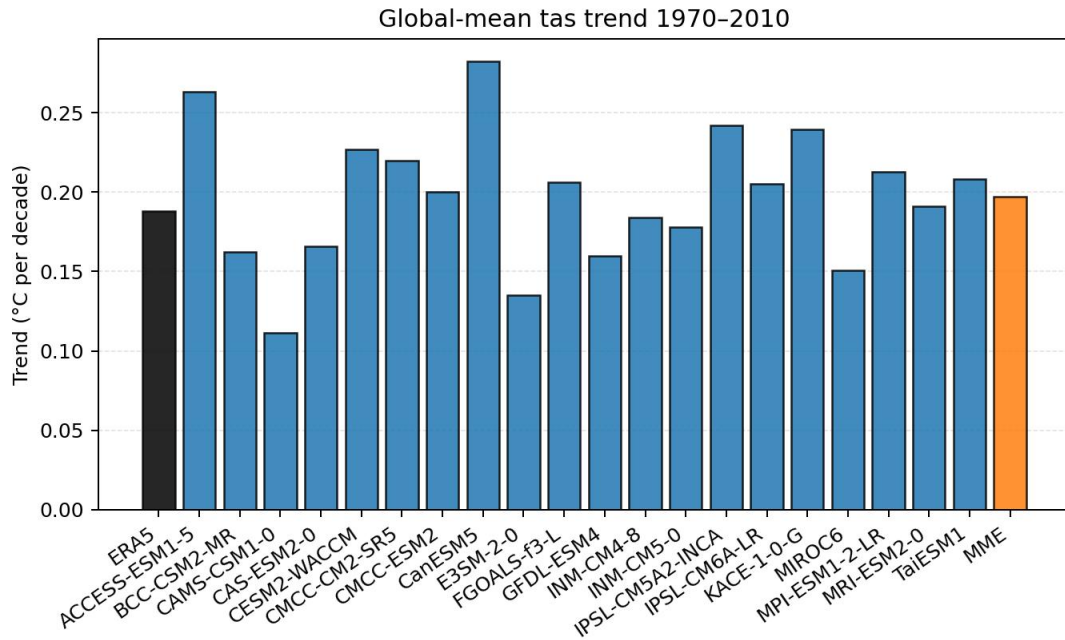
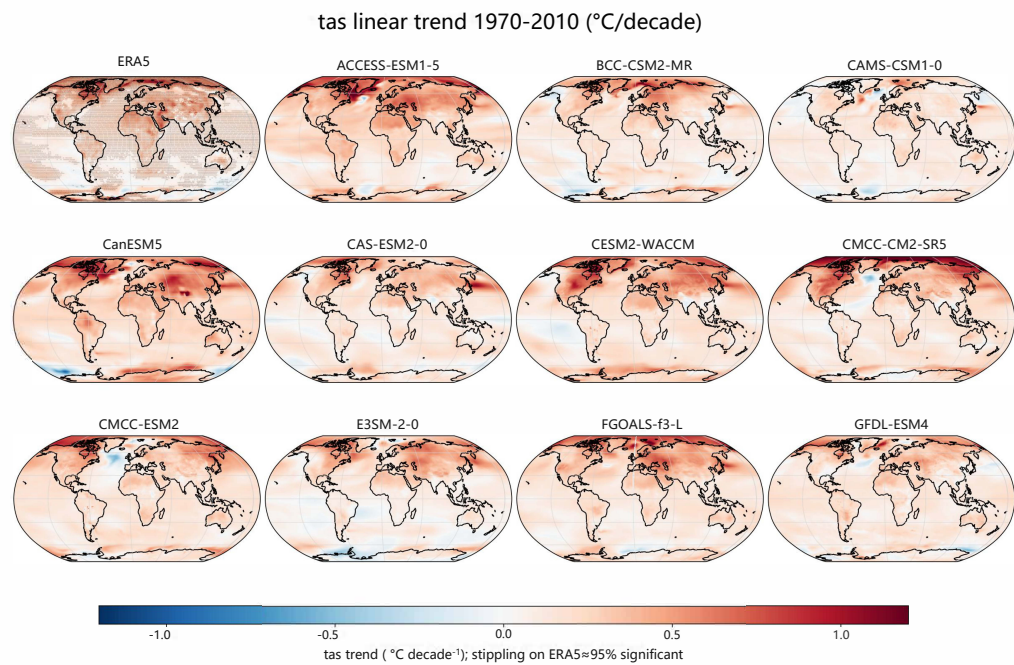


Figure 7 | Automated Climate Analysis - Temperature Trends. InternAgent-1.5 autonomously generated this diagnostic for 20 CMIP6 models against ERA5 (1970-2010), showing the ranked bar chart of global-mean temperature trends (°C/decade).

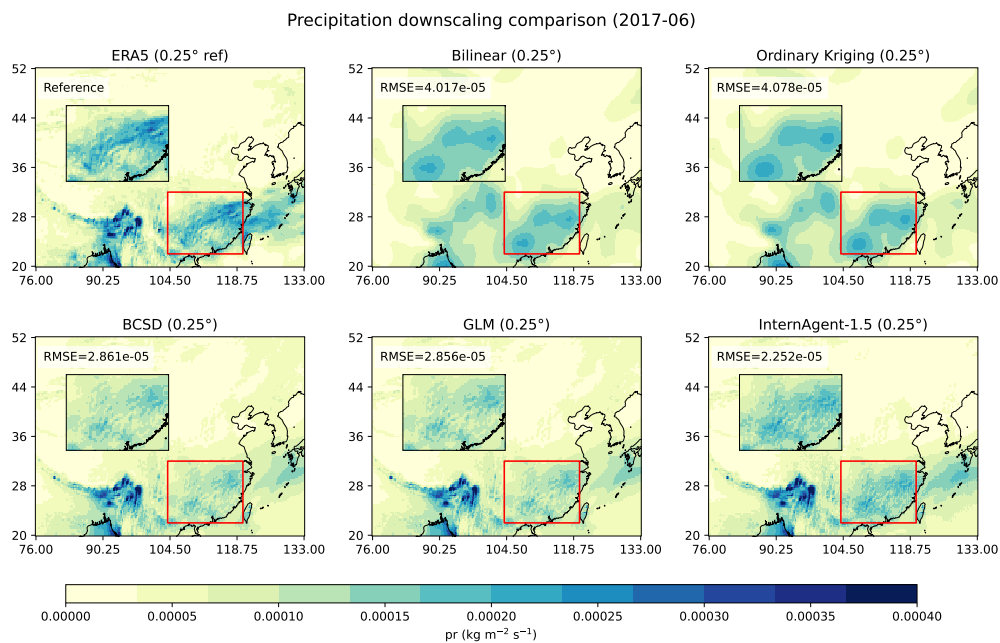
Building on the setup described in Sec. 3.1, we demonstrate how InternAgent-1.5 addresses the dual challenges of knowledge integration and high-fidelity modeling in Earth Science.

Automated Data Analysis and Knowledge Integration. In the *Automated Climate Diagnostics* task, the system was prompted to evaluate CMIP6 climate model simulations against the ERA5 reanalysis. Rather than simply calculating statistics, InternAgent-1.5 employed its *Knowledge Flow Planner* to integrate climate modeling literature and physical reasoning. Guided by widely adopted diagnostic conventions, the system selected key evaluation metrics, including global-mean surface temperature trends (°C decade⁻¹) and model–observation biases, and constructed an end-to-end analysis pipeline encompassing data retrieval, temporal alignment, and statistical estimation.

The system successfully processed the multi model ensemble and generated a ranked bar chart in Fig. 7 that contextualizes model performance. To further assess the physical consistency of the simulated trends, InternAgent-1.5 also produced spatial maps of linear temperature change in Fig. 8, which enable interpretation at the regional scale. These diagnostics reveal canonical large scale warming patterns, including enhanced high latitude trends that match established characteristics of observed and simulated climate change. Taken together, the results show that InternAgent-1.5 supports climate analysis not only by automating computation but also by organizing diagnostics in a manner that aligns with domain specific interpretability.



(a)



(b)

Figure 8 | (a) Automated Climate Analysis - Spatial Patterns. Spatial maps of linear temperature trends generated by InternAgent-1.5, identifying regional warming patterns across different CMIP6 models. (b) Precipitation downscaling comparison across different methods.

Algorithmic Innovation and Optimization. For the *Climate Downscaling Optimization* task, InternAgent-1.5 addressed known limitations of widely used baseline methods, including Kriging [55] and BCSD [56], which can struggle to represent non-stationary biases and fine-scale spatial variability in surface temperature fields.

The system autonomously conducted a literature review, recognizing that standard linear assumptions are insufficient for non-stationary biases. It proposed a deep-learning-based approach designed to capture complex spatial dependencies, generated the implementation code, and refined the architecture through iterative validation. As shown in Fig. 8 and summarized in Table 9, the model optimized by InternAgent-1.5 achieves improved performance relative to established statistical baselines. While the baseline Kriging and BCSD methods yielded RMSEs of 3.1658 and 0.9049 respectively, our system's solution reduced the RMSE to **0.8488**.

Beyond improvements in bulk error statistics, qualitative comparison of spatial fields indicates that bilinear interpolation and kriging introduce substantial spatial smoothing and attenuate high-intensity precipitation cores. In contrast, the InternAgent-1.5 more faithfully reproduces fine-scale spatial gradients and localized convective maxima present in the ERA5 reference data. This suggests that the model effectively captures nonlinear and scale-interactive processes that are not resolved by conventional interpolation or stationary bias-correction methods. Collectively, these results confirms that InternAgent-1.5 can independently conceive and optimize new scientific tools rather than merely applying existing ones.

Table 9 | Performance Comparison on Climate Downscaling Task. The deep learning method proposed and implemented by InternAgent-1.5 outperforms both traditional interpolation and statistical correction baselines in reconstructing high-resolution (0.25°) surface temperature fields.

Method	Type	RMSE
Kriging Interpolation	Traditional Spatial	3.1658
BCSD	Statistical Correction	0.9049
InternAgent-1.5	AI-Optimized Deep Learning	0.8488

3.4.2. Life Science

We present two representative case studies to illustrate how InternAgent-1.5 supports therapeutic target discovery in realistic biomedical scenarios.

Automated Biological Evidence Synthesis. As a case study, we reproduced the discovery of *GPR160* as a novel therapeutic target in hepatocellular carcinoma (HCC) reported by OriGene [83]. We prompted InternAgent-1.5 to “identify understudied yet mechanistically promising druggable targets in HCC using multi-modal evidence.”

Using the *Knowledge Flow Planner*, the system autonomously decomposed the task into differential expression analysis, mutation and copy-number evaluation, survival association testing, pathway enrichment, and tractability assessment. It queried canonical resources including GEPIA, TCGA, GEO, and OpenTargets to generate an initial pool of 125 candidate genes, which was progressively narrowed to *GPR160* through multi-round evidence compression and reflection. The system further produced expression profiles, Kaplan–Meier survival curves, and KEGG pathway maps, revealing tumor-specific overexpression of *GPR160*, its association with poor recurrence-free survival, and its potential involvement in immune-related signaling. This case demonstrates InternAgent-1.5’s ability to translate open-ended biomedical questions into structured and mechanistically grounded evidence chains.

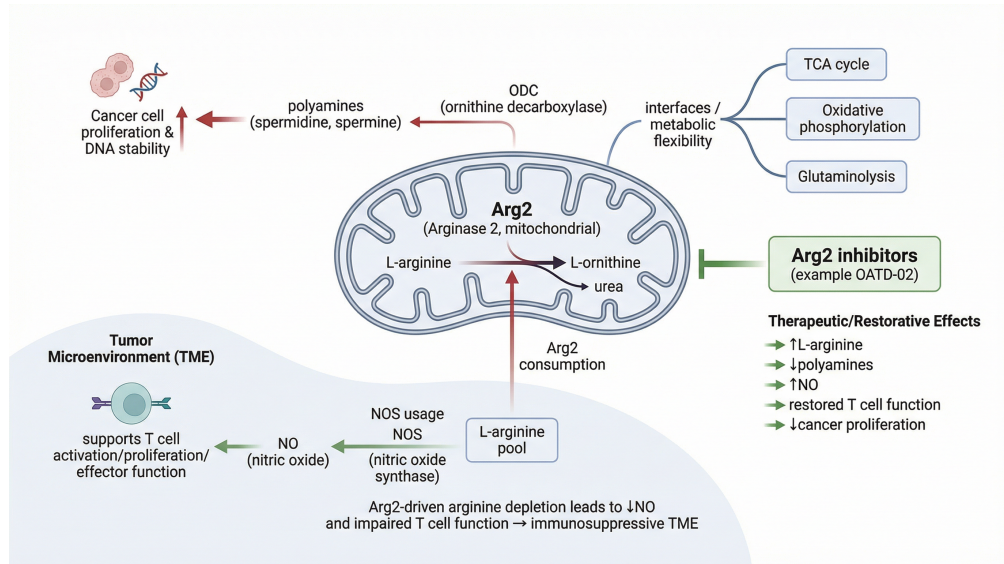


Figure 9 | Mitochondrial Arg2 immunometabolic pathway and therapeutic intervention points

Hypothesis Generation and Target Prioritization. We further reproduced the identification of *ARG2* as an overlooked yet mechanistically grounded target in colorectal cancer (CRC). The system constructed a multi-modal evidence graph integrating TCGA cohorts, Human Protein Atlas proteomics, UCSC genome annotations, pathway knowledge, and literature-derived molecular mechanisms. Built upon domain-specific reasoning templates, InternAgent-1.5 executed structured reasoning steps including disease gene consistency checks, pathway–phenotype alignment, pharmacological tractability analysis, and clinical differential expression testing.

Through iterative reflection cycles, *ARG2* emerged as the top-ranked candidate, accompanied by mechanistic explanations involving metabolic reprogramming and immunosuppressive microenvironment remodeling. As illustrated in Fig. 9, which is automatically generated by InternAgent-1.5, mitochondrial *ARG2*-driven arginine depletion reduces nitric oxide (NO) availability, impairs T-cell effector function, and promotes tumor proliferation via enhanced polyamine biosynthesis, providing a unified metabolic–immunological rationale for therapeutic intervention. The complete report is released in our open-source repository.

InternAgent-1.5 further generated experiment-ready recommendations, including dose–response assays, patient-derived organoid (PDO) validation, and immune profiling protocols, consistent with those used in the original study. Notably, *ARG2* inhibition exhibited dose-dependent anti-tumor effects in HCT116 cells and multiple CRC PDO models, supporting the validity of the generated hypotheses.

Together, these case studies show that InternAgent-1.5 can support end-to-end target discovery, bridging multi-omics evidence integration, mechanistic hypothesis generation, and experimental guidance.

3.4.3. Biological Science

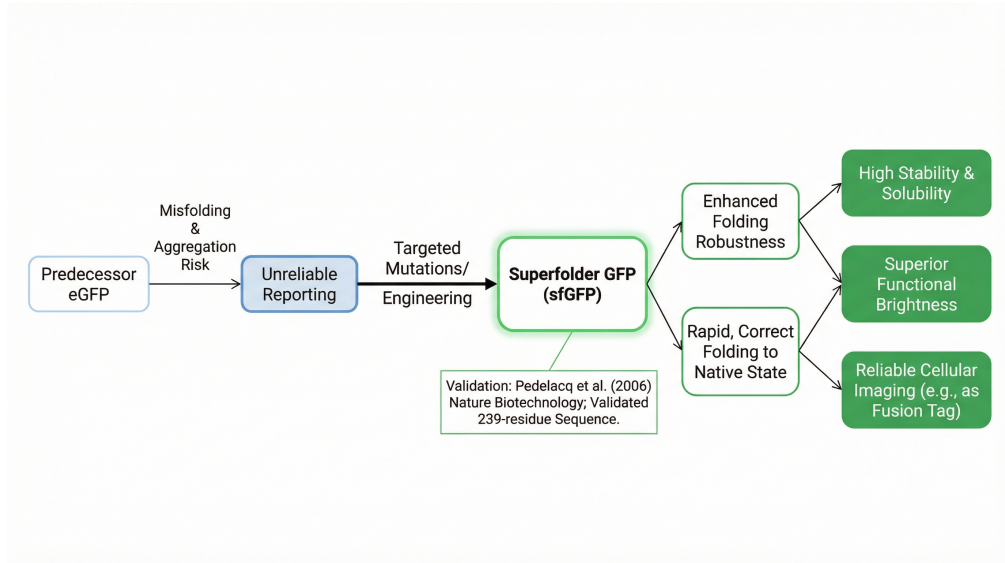


Figure 10 | The engineering evolution from eGFP to sfGFP

The experimental began with a targeted literature search by InternAgent-1.5 to identify fluorescent protein variants with strong brightness and folding stability. Evidence from peer reviewed studies pointed to sfGFP as a suitable candidate. This information, combined with predefined performance objectives, guided the design of the computational analyses and the experimental validation plan.

To evaluate these candidates, a series of dry lab and wet lab procedures were carried out using tools and devices coordinated through SCP [32]. The workflow included fluorescence assays, stability measurements, and quality control checks, paired with dry lab predictions of structural stability and sequence function relationships. The results show that sfGFP achieves high functional brightness and reliable folding efficiency, consistent with findings reported in the literature. Based on all data returned by SCP coordinated tools and instruments, InternAgent-1.5 generated a final experimental report that summarizes the empirical outcomes and identifies variants appropriate for downstream use. Figure 10, which is automatically generated by InternAgent-1.5, presents an intermediate reasoning artifact automatically produced by InternAgent-1.5, which outlines how evidence from the literature is transformed into an engineering rationale and target selection for sfGFP, and the complete report is available in our open source repository.

3.4.4. Physical Science

Building on the setup described in Sec. 3.1, we demonstrate how InternAgent-1.5 addresses the dual challenges of strict atomic conservation and vast chemical search spaces in Physical Science. We report quantitative metrics on reaction prediction benchmarks and qualitative case studies in generative drug design.

Table 10 | Performance on Forward Major Product (Fwd_{major}) and By-product Prediction (Fwd_{by}). Top-1 accuracy and Fingerprint Tanimoto Similarity (FTS) are reported.

Models	Fwd_{major}		Fwd_{by}	
	Top-1	FTS ↑	Top-1	FTS ↑
GPT-5.2	59	0.79	45	0.40
Claude4.5-sonnet-think	0.74	0.90	0.49	0.43
o3-mini	0.55	0.74	0.47	0.47
Gemini-3-Pro-Thinking	0.81	0.91	0.45	0.36
InternAgent-1.5	0.86	0.94	0.62	0.42

Automated Reaction Outcome Prediction. We evaluated the system on the ChemCoTBench [62] forward prediction task. Unlike standard language models that treat molecular strings as mere text [84], InternAgent-1.5 adopts a physicochemical-aware approach by proactively invoking RD-Kit [85] to compute critical molecular descriptors (e.g., LogP, TPSA) and standardize SMILES representations. This descriptor-guided reasoning allows the system to accurately deduce the main product while simultaneously employing atomic conservation logic to infer by-products such as water or halides. As detailed in Table 10, InternAgent-1.5 achieves a Top-1 accuracy of 0.86 and a Fingerprint Tanimoto Similarity (FTS) of 0.94 for major product prediction. These results significantly outperform recent reasoning-enhanced models such as o3-mini (Top-1 0.55) and Gemini-3-Pro-Thinking (Top-1 0.81). Furthermore, in the challenging by-product prediction task (Fwd_{by}), our system achieves the highest Top-1 accuracy of 0.62, confirming its robustness in capturing complete reaction stoichiometry.

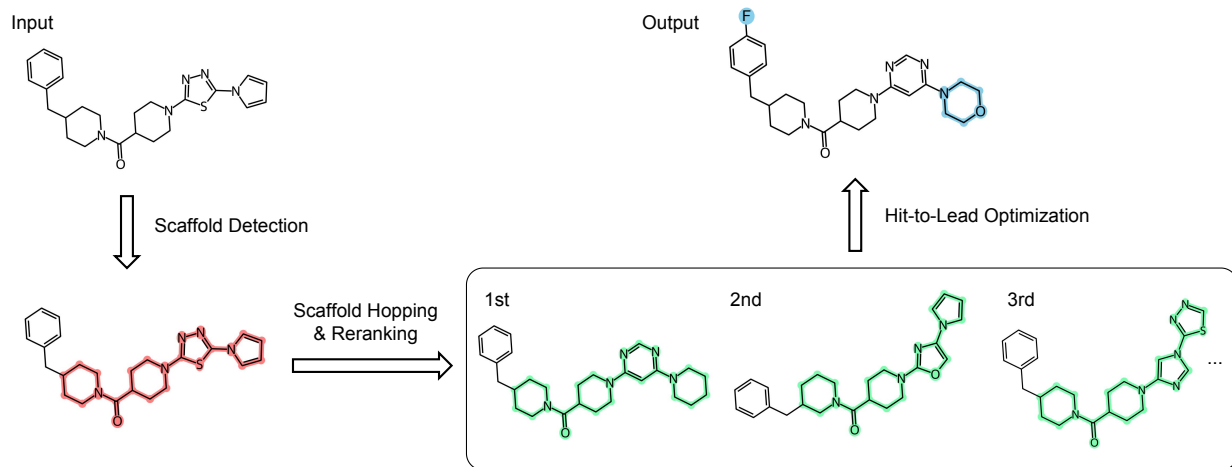


Figure 11 | **Automated scaffold hopping and hit to lead optimization using InternAgent-1.5.** The workflow begins by identifying the core scaffold in red from a DprE1 inhibitor hit. Through coordinated agent interaction, the system proposes structurally diverse bioisosteres and prioritizes piperidinopyrimidine variants shown in green. It then conducts a focused optimization step to address physicochemical limitations and generates a final candidate highlighted in blue, which features a modified heterocycle and fluorination. The resulting trajectory follows established medicinal chemistry practice and demonstrates the system’s ability to support rational drug design.

Generative Scaffold Hopping. In the drug design domain, InternAgent-1.5 employs a generative multi-agent workflow that prioritizes 3D shape and electrostatic alignment over simple 2D topology.

Crucially, the system integrates agent reasoning to refine candidates based on calculated metrics including Synthetic Accessibility (SA), Tanimoto Similarity, and LogP. When applied to a DprE1 inhibitor template known for solubility limitations [86], the agent successfully navigated away from the original pyrrolothiadiazole core, proposing plausible bioisosteres based on piperidinopyrimidine scaffolds (Figure 11, Outputs 1st–3rd). Notably, the agent autonomously simulated a “hit-to-lead” optimization phase. It replicated expert-driven evolution by replacing the lipophilic piperidine side chain with a polar morpholine ring and introducing a fluorine atom at the para-position of the phenyl ring (Output), modifications critical for enhancing metabolic stability and solubility [86].

3.5. Effectiveness of Structured Cognitive Memory

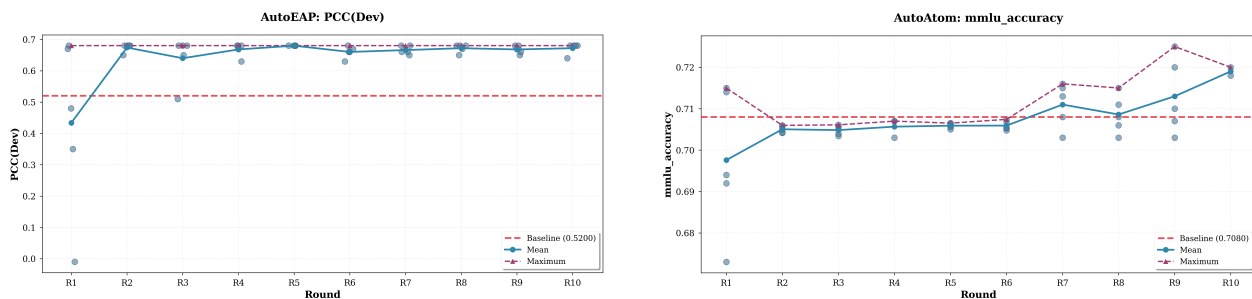


Figure 12 | Experimental validation of memory effectiveness on algorithm discovery tasks.

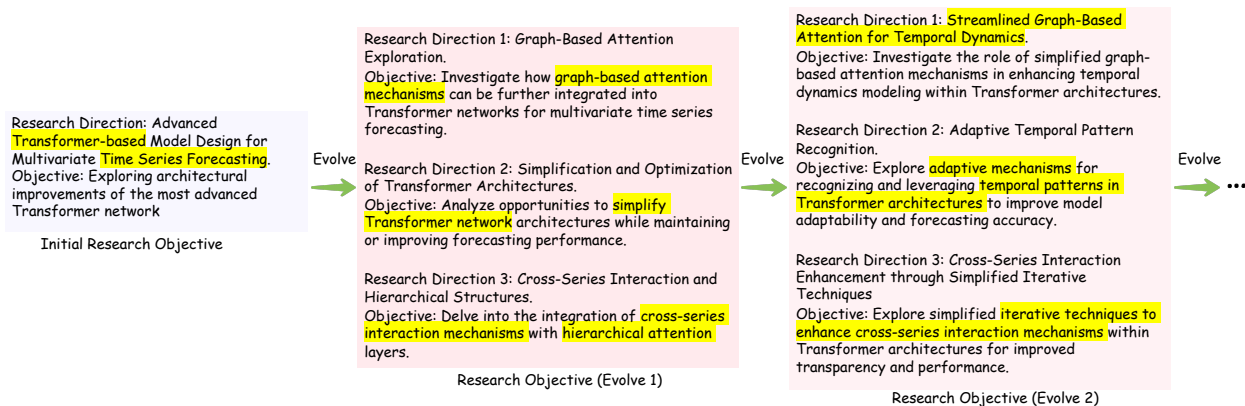


Figure 13 | The evolution process of research objectives on the AutoTSF task.

Our system is designed to operate continuously over extended periods, and the Structured Cognitive Memory subsystem is a core component that enables sustained improvement across diverse scientific discovery tasks. To isolate how each module contributes to long-horizon capability, we evaluate Task-Episodic Memory (TEM), Semantic-Knowledge Memory (SKM), and Strategy-Procedural Memory (SPM) using modalities aligned with their functional roles.

Task-Episodic Memory. We analyze TEM through performance trajectories over iterative research steps. With TEM active, curves rise smoothly, indicating stable short-horizon adaptation. Retrieved episodes provide fine-grained evidence from earlier trials, helping the model avoid ineffective methodological choices and refine hypotheses efficiently. Removing TEM yields irregular or stagnant progression, with frequent revisiting of unproductive strategies due to missing within-session outcomes. This contrast shows episodic grounding is critical for robust, sample-efficient adaptation during sustained operation. Fig.12 further presents long-horizon optimization experiments on scientific-discovery tasks, illustrating how TEM supports stable and persistent iterative improvement.

Table 11 | Ablation study on the strategy-procedural memory on the GAIA benchmark. We report accuracy and the average of tool calls to evaluate both performance and efficiency.

Agent	GAIA Accuracy (%) ↑				Avg. # Tool Calls ↓			
	Level 1	Level 2	Level 3	Avg.	Level 1	Level 2	Level 3	Avg.
InternAgent 1.5 w/o SPM	92.45	84.88	53.85	82.42	12.06	23.51	55.65	22.69
InternAgent 1.5	92.45	89.53	61.54	86.06	9.13	21.22	37.33	18.52

Semantic-Knowledge Memory. To assess SKM, we use prompt-based case studies where the system proposes new research directions after multiple exploration batches. With SKM enabled, objectives reflect accumulated understanding of successful and unsuccessful methodological patterns. Retrieved long-term knowledge helps avoid saturated conceptual regions while preserving semantic continuity and measurable novelty. Fig. 13 illustrates iterative evolution of research objectives from an initial seed, showing that SKM maintains cross-batch coherence while allowing strategic redundancy to deepen promising sub-domains, balancing exploration breadth with exploitation depth.

Strategy-Procedural Memory. As shown in Table 11, we evaluate SPM on benchmark tasks requiring multi-step reasoning and coordinated planning. The full system achieves higher success rates and more coherent plans than the SPM-ablated baseline. SPM provides procedural priors that improve planning structure and execution-level tool selection, reducing unnecessary branching and redundant calls. Without SPM, plans become longer and fragmented, with error propagation and imprecise tool-call parameters. Overall, SPM supports transferable procedural structure and improves planning efficiency and execution rigor.

Overall, TEM, SKM, and SPM provide complementary support across short-term adaptation, long-term knowledge accumulation, and efficient reasoning execution for sustained improvement.

4. Related Work

4.1. Agentic AI for Scientific Discovery

Recent progress in agentic AI has produced systems capable of carrying out increasingly autonomous forms of scientific reasoning. The AI Scientist [1] line of work demonstrates early examples of end to end research automation, with the initial system coordinating hypothesis generation and experiment design, and the later version [2] replacing fixed templates with a search based procedure that allows broader exploration of methodological space. AlphaEvolve [3] approaches scientific discovery from an evolutionary perspective by using language models to generate candidate algorithms and iteratively refine them through performance guided optimization. Other recent systems emphasize multi agent coordination within real scientific workflows. AI Co-Scientist [4] distributes literature analysis, hypothesis refinement, and methodological planning across specialized agents directed by a central model, while Robin integrates planning, data analysis, and validation into a closed loop system capable of discovering new compound candidates without manual intervention. Kosmos [6] further advances this direction by unifying literature retrieval, experiment design, and theory development into a continuously running discovery engine. Overall, these efforts illustrate the rapid emergence of autonomous scientific discovery systems and highlight the importance of long horizon reasoning, iterative experimentation, and persistent state management. These themes directly motivate the structured memory mechanisms developed in our work.

4.2. Deep Research Agents

Recent advances in Deep Research (DR) agents extend LLMs from retrieval-augmented generation to dynamic, tool-driven research workflows. Early systems such as WebGPT [87] and Toolformer [88] explored web and API integration, demonstrating how models can reason over retrieved information while selectively invoking external tools. Building on these ideas, industrial solutions *e.g.*, OpenAI DR [72], Gemini DR [75], Grok DR [89], and Perplexity DR [90], incorporate adaptive planning, iterative retrieval, and multimodal reasoning to support long-horizon research tasks. Recently, single-agent designs (*e.g.*, Search-o1 [91], WebDancer [68], Tongyi DeepResearcher [92], MiroThinker [70]) enable end-to-end optimization within a unified reasoning loop, while multi-agent architectures (*e.g.*, AI Scientist [1], Agent Laboratory [93], and InternAgent [7]) offer greater modularity and scalability, which are particularly beneficial for complex research settings. Recent studies, *e.g.*, GeAR [94] and PANGU DeepDiver [95], further demonstrate the value of explicit structures and self-evolving mechanisms for multi-hop reasoning.

4.3. Memory Mechanism

Agent memory has become a central component of modern agent systems, enabling long-horizon reasoning, continual adaptation, and interaction with complex environments [96]. Recent advances cover token-level mechanisms [97] that extend contextual retention, parametric approaches that internalize accumulated experience into model parameters, and latent-memory systems [98] that store structured trajectories to guide future decisions. In parallel, short-term interaction memory has been explored in conversational and agent-simulation settings, where systems maintain ephemeral contextual traces to support local reasoning over brief episodes [99]. Long-term episodic memory has also been investigated through architectures that accumulate environment interactions across extended horizons and retrieve them for subsequent decisions [48], providing persistent records of agent experience. These techniques enhance an agent's mechanisms for incorporating prior information, although they are typically designed for interaction settings with limited temporal scope and therefore remain orthogonal to the multi-stage workflows considered in scientific discovery.

5. Conclusion

In this work, we presented InternAgent-1.5, a unified system for end-to-end scientific discovery. The framework integrates generation, verification, and evolution into a coherent architecture supported by foundational capabilities for deep research, solution refinement, and long horizon memory. This design enables consistent information flow across stages and provides a general substrate for cross-disciplinary scientific workflows.

Comprehensive evaluations demonstrate that InternAgent-1.5 achieves strong performance in structured scientific reasoning. The system autonomously produces competitive algorithmic solutions, optimizes experimental proposals over extended trajectories, and executes multi-step computational and empirical workflows. Across algorithmic and empirical domains, InternAgent-1.5 consistently generates outputs that align with established scientific principles and reproduce findings observed in real scientific studies.

Future work includes strengthening the coupling between computational reasoning and experimental validation, and accelerating the transition from generated hypotheses to verifiable results. Advancing these directions will further improve the efficiency and reliability of cross-disciplinary scientific discovery.

References

- [1] Chris Lu et al. “The ai scientist: Towards fully automated open-ended scientific discovery”. In: *arXiv preprint arXiv:2408.06292* (2024).
- [2] Yutaro Yamada et al. “The ai scientist-v2: Workshop-level automated scientific discovery via agentic tree search”. In: *arXiv preprint arXiv:2504.08066* (2025).
- [3] Alexander Novikov et al. “AlphaEvolve: A coding agent for scientific and algorithmic discovery”. In: *arXiv preprint arXiv:2506.13131* (2025).
- [4] Juraj Gottweis et al. “Towards an AI co-scientist”. In: *arXiv preprint arXiv:2502.18864* (2025).
- [5] Ali Essam Ghareeb et al. “Robin: A multi-agent system for automating scientific discovery”. In: *arXiv preprint arXiv:2505.13400* (2025).
- [6] Ludovico Mitchener et al. “Kosmos: An AI Scientist for Autonomous Discovery”. In: *arXiv preprint arXiv:2511.02824* (2025).
- [7] NovelSeek Team et al. “NovelSeek: When Agent Becomes the Scientist–Building Closed-Loop System from Hypothesis to Verification”. In: *arXiv preprint arXiv:2505.16938* (2025).
- [8] Hanchen Wang et al. “Scientific discovery in the age of artificial intelligence”. In: *Nature* 620.7972 (2023), pp. 47–60.
- [9] Richard Van Noorden and Jeffrey M Perkel. “AI and science: what 1,600 researchers think”. In: *Nature* 621.7980 (2023), pp. 672–675.
- [10] Josh Abramson et al. “Accurate structure prediction of biomolecular interactions with AlphaFold 3”. In: *Nature* 630.8016 (2024), pp. 493–500.
- [11] John Jumper et al. “Highly accurate protein structure prediction with AlphaFold”. In: *nature* 596.7873 (2021), pp. 583–589.
- [12] Mihaly Varadi et al. “AlphaFold Protein Structure Database: massively expanding the structural coverage of protein-sequence space with high-accuracy models”. In: *Nucleic acids research* 50.D1 (2022), pp. D439–D444.
- [13] Andres M. Bran et al. “Augmenting large language models with chemistry tools”. In: *Nature Machine Intelligence* 6.5 (2024), pp. 525–535.
- [14] Zijie Guo et al. “EarthLink: A Self-Evolving AI Agent for Climate Science”. In: *arXiv preprint arXiv:2507.17311* (2025).
- [15] Bernard J Jansen, Soon-gyo Jung, and Joni Salminen. “Employing large language models in survey research”. In: *Natural Language Processing Journal* 4 (2023), p. 100020.
- [16] Xiangchao Yan et al. “Surveyforge: On the outline heuristics, memory-driven generation, and multi-dimensional evaluation for automated survey writing”. In: *Proceedings of the 63rd Annual Meeting of the Association for Computational Linguistics (Volume 1: Long Papers)*. 2025, pp. 12444–12465.
- [17] Biqing Qi et al. “Large language models are zero shot hypothesis proposers”. In: *arXiv preprint arXiv:2311.05965* (2023).
- [18] Biqing Qi et al. “Large language models as biomedical hypothesis generators: a comprehensive evaluation”. In: *arXiv preprint arXiv:2407.08940* (2024).
- [19] Shangheng Du et al. “AutoMLGen: Navigating Fine-Grained Optimization for Coding Agents”. In: *arXiv preprint arXiv:2510.08511* (2025).
- [20] Yusong Hu et al. “FlowSearch: Advancing deep research with dynamic structured knowledge flow”. In: *arXiv preprint arXiv:2510.08521* (2025).

- [21] Jiakang Yuan et al. “Dolphin: moving towards closed-loop auto-research through thinking, practice, and feedback”. In: *Proceedings of the 63rd Annual Meeting of the Association for Computational Linguistics (Volume 1: Long Papers)*. 2025, pp. 21768–21789.
- [22] Adib Bazgir, Yuwen Zhang, et al. “Agentichypothesis: A survey on hypothesis generation using llm systems”. In: *Towards Agentic AI for Science: Hypothesis Generation, Comprehension, Quantification, and Validation* (2025).
- [23] Mario Bunge. *Scientific Research. 2 Volumes*. 1967.
- [24] Tony Hey, Stewart Tansley, Kristin Michele Tolle, et al. *The fourth paradigm: data-intensive scientific discovery*. Vol. 1. Microsoft research Redmond, WA, 2009.
- [25] Grégoire Mialon et al. “Gaia: a benchmark for general ai assistants”. In: *International Conference on Learning Representations (ICLR)*. 2023.
- [26] David Rein et al. “Gpqa: A graduate-level google-proof q&a benchmark”. In: *First Conference on Language Modeling*. 2024.
- [27] Long Phan et al. “Humanity’s last exam”. In: *arXiv preprint arXiv:2501.14249* (2025).
- [28] OpenAI. *FrontierScience: Evaluating AI’s Ability To Perform Expert-level Scientific Tasks*. <https://openai.com/index/frontierscience/>. 2026.
- [29] Wanghan Xu et al. “Probing Scientific General Intelligence of LLMs with Scientist-Aligned Workflows”. In: *arXiv preprint arXiv:2512.16969* (2025).
- [30] Ines Chami et al. “Low-Dimensional Hyperbolic Knowledge Graph Embeddings”. In: *Annual Meeting of the Association for Computational Linguistics*. 2020, pp. 6901–6914.
- [31] Zongsheng Cao et al. “DiffusionE: Reasoning on Knowledge Graphs via Diffusion-based Graph Neural Networks”. In: *ACM SIGKDD Conference on Knowledge Discovery and Data Mining*. 2024, pp. 222–230.
- [32] Yankai Jiang et al. “SCP: Accelerating Discovery with a Global Web of Autonomous Scientific Agents”. In: *arXiv preprint arXiv:2512.24189* (2025).
- [33] Paul Gauthier and Aider-AI Contributors. *Aider: AI pair programming in your terminal*. <https://github.com/Aider-AI/aider>. Accessed: 2025-05-07. 2023. URL: <https://github.com/Aider-AI/aider>.
- [34] Yixin Ou et al. “AutoMind: Adaptive Knowledgeable Agent for Automated Data Science”. In: *arXiv preprint arXiv:2506.10974* (2025).
- [35] Damith Perera et al. “A platform for automated nanomole-scale reaction screening and micromole-scale synthesis in flow”. In: *Science* 359.6374 (2018), pp. 429–434.
- [36] Abhimanyu Dubey et al. “The llama 3 herd of models”. In: *arXiv e-prints* (2024), arXiv-2407.
- [37] Thomas M Norman et al. “Exploring genetic interaction manifolds constructed from rich single-cell phenotypes”. In: *Science* 365.6455 (2019), pp. 786–793.
- [38] Yusuf Roohani, Kexin Huang, and Jure Leskovec. “Predicting transcriptional outcomes of novel multigene perturbations with GEARS”. In: *Nature Biotechnology* 42.6 (2024), pp. 927–935.
- [39] Ray Daniel Zimmerman, Carlos Edmundo Murillo-Sánchez, and Robert John Thomas. “MAT-POWER: Steady-state operations, planning, and analysis tools for power systems research and education”. In: *IEEE Transactions on power systems* 26.1 (2010), pp. 12–19.
- [40] Zhen Zhao et al. “SenseFlow: A Physics-Informed and Self-Ensembling Iterative Framework for Power Flow Estimation”. In: *arXiv preprint arXiv:2505.12302* (2025).

[41] Haoyi Zhou et al. “Informer: Beyond Efficient Transformer for Long Sequence Time-Series Forecasting”. In: *The Thirty-Fifth AAAI Conference on Artificial Intelligence, AAAI 2021, Virtual Conference*. Vol. 35. 12. AAAI Press, 2021, pp. 11106–11115.

[42] Ailing Zeng et al. “Are transformers effective for time series forecasting?” In: *Proceedings of the AAAI conference on artificial intelligence*. Vol. 37. 9. 2023, pp. 11121–11128.

[43] Stefan Chmiela et al. “Machine learning of accurate energy-conserving molecular force fields”. In: *Science advances* 3.5 (2017), e1603015.

[44] Yusong Wang et al. “Enhancing geometric representations for molecules with equivariant vector-scalar interactive message passing”. In: *Nature Communications* 15.1 (2024), p. 313.

[45] Cosmas D Arnold et al. “Genome-wide quantitative enhancer activity maps identified by STARR-seq”. In: *Science* 339.6123 (2013), pp. 1074–1077.

[46] Bernardo P de Almeida et al. “DeepSTARR predicts enhancer activity from DNA sequence and enables the de novo design of synthetic enhancers”. In: *Nature genetics* 54.5 (2022), pp. 613–624.

[47] Fengwei Teng et al. “Atom of Thoughts for Markov LLM Test-Time Scaling”. In: *The Thirty-ninth Annual Conference on Neural Information Processing Systems*. 2025.

[48] Wujiang Xu et al. “A-Mem: Agentic Memory for LLM Agents”. In: *The Thirty-ninth Annual Conference on Neural Information Processing Systems*. 2025. URL: <https://openreview.net/forum?id=FiMOM8gcct>.

[49] Zheng Cai et al. *InternLM2 Technical Report*. 2024. arXiv: [2403.17297 \[cs.CL\]](https://arxiv.org/abs/2403.17297).

[50] Jia Li et al. “Numinamath: The largest public dataset in ai4maths with 860k pairs of competition math problems and solutions”. In: *Hugging Face repository* 13.9 (2024), p. 9.

[51] Yuxin Zuo et al. “TTRL: Test-Time Reinforcement Learning”. In: *The Thirty-ninth Annual Conference on Neural Information Processing Systems*. 2025. URL: [https://openreview.net/forum?id=VuVhgEiu20&referrer=%5Bthe%20profile%20of%20Bowen%20Zhou%5D\(%2Fprofile%3Fid%3D~Bowen_Zhou8\)](https://openreview.net/forum?id=VuVhgEiu20&referrer=%5Bthe%20profile%20of%20Bowen%20Zhou%5D(%2Fprofile%3Fid%3D~Bowen_Zhou8)).

[52] Veronika Eyring et al. “Overview of the Coupled Model Intercomparison Project Phase 6 (CMIP6) experimental design and organization”. In: *Geoscientific Model Development* 9.5 (2016), pp. 1937–1958.

[53] Hans Hersbach et al. “ERA5 monthly averaged data on single levels from 1979 to present”. In: *Copernicus Climate Change Service (C3S) Climate Data Store (CDS)* 10 (2019), pp. 252–266.

[54] Eugenia Kalnay et al. “The NCEP/NCAR 40-year reanalysis project”. In: *Renewable energy*. Routledge, 2018, Vol1_146–Vol1_194.

[55] Tomislav Hengl, Gerard BM Heuvelink, and David G Rossiter. “About regression-kriging: From equations to case studies”. In: *Computers & geosciences* 33.10 (2007), pp. 1301–1315.

[56] Andrew W Wood et al. “Long-range experimental hydrologic forecasting for the eastern United States”. In: *Journal of Geophysical Research: Atmospheres* 107.D20 (2002), ACL–6.

[57] Katarzyna Tomczak, Patrycja Czerwińska, and Maciej Wiznerowicz. “Review The Cancer Genome Atlas (TCGA): an immeasurable source of knowledge”. In: *Contemporary Oncology/Współczesna Onkologia* 2015.1 (2015), pp. 68–77.

[58] Denise Carvalho-Silva et al. “Open Targets Platform: new developments and updates two years on”. In: *Nucleic acids research* 47.D1 (2019), pp. D1056–D1065.

[59] Minoru Kanehisa. “The KEGG database”. In: *In silico’simulation of biological processes: Novartis Foundation Symposium* 247. Vol. 247. Wiley Online Library. 2002, pp. 91–103.

[60] Alexander Rives et al. “Biological Structure and Function Emerge from Scaling Unsupervised Learning to 250 Million Protein Sequences”. In: *PNAS* (2019). doi: [10.1101/622803](https://doi.org/10.1101/622803). URL: <https://www.biorxiv.org/content/10.1101/622803v4>.

[61] Mingchen Li et al. “ProSST: Protein Language Modeling with Quantized Structure and Disentangled Attention”. In: *The Thirty-eighth Annual Conference on Neural Information Processing Systems*. 2024.

[62] Hao Li et al. “Beyond Chemical QA: Evaluating LLM’s Chemical Reasoning with Modular Chemical Operations”. In: *arXiv preprint arXiv:2505.21318* (2025).

[63] *Gemini 3 Pro - Google DeepMind*. URL: <https://deepmind.google/models/gemini/pro/>.

[64] OpenAI. *ChatGPT (GPT-5)*. 2025. URL: <https://chat.openai.com/>.

[65] *Introducing Claude Sonnet 4.5*. en. URL: <https://www.anthropic.com/news/claudesonnet-4-5>.

[66] An Yang et al. “Qwen3 technical report”. In: *arXiv preprint arXiv:2505.09388* (2025).

[67] *Introducing OpenAI o3 and o4-mini*. en-US. URL: <https://openai.com/index/introducing-o3-and-o4-mini/>.

[68] Jialong Wu et al. “WebDancer: Towards Autonomous Information Seeking Agency”. In: *arXiv preprint arXiv:2505.22648* (2025).

[69] Zhengwei Tao et al. “Webshaper: Agentically data synthesizing via information-seeking formalization”. In: *arXiv preprint arXiv:2507.15061* (2025).

[70] MiroMind Team et al. “MiroThinker: Pushing the Performance Boundaries of Open-Source Research Agents via Model, Context, and Interactive Scaling”. In: *arXiv preprint arXiv:2511.11793* (2025).

[71] Tongyi DeepResearch Team et al. “Tongyi DeepResearch Technical Report”. In: *arXiv preprint arXiv:2510.24701* (2025).

[72] OpenAI. *Deep Research System Card*. <https://cdn.openai.com/deep-research-system-card.pdf>. 2025.

[73] Moonshot AI. *Kimi-Researcher: End-to-End Reinforcement Learning for Emerging Agentic Capabilities*. <https://moonshotai.github.io/Kimi-Researcher/>. Accessed: 2025-XX-XX. 2025.

[74] *Manus*. <https://manus.im/>. 2025.

[75] Google. *Introducing Gemini Deep Research*. <https://blog.google/products/gemini/google-gemini-deep-research/>. 2024.

[76] Mengkang Hu et al. *OWL: Optimized Workforce Learning for General Multi-Agent Assistance in Real-World Task Automation*. 2025. arXiv: [2505.23885 \[cs.AI\]](https://arxiv.org/abs/2505.23885).

[77] Daya Guo et al. “Deepseek-r1: Incentivizing reasoning capability in llms via reinforcement learning”. In: *arXiv preprint arXiv:2501.12948* (2025).

[78] Lei Bai et al. “Intern-s1: A scientific multimodal foundation model”. In: *arXiv preprint arXiv:2508.15763* (2025).

[79] Aixin Liu et al. “Deepseek-v3. 2: Pushing the frontier of open large language models”. In: *arXiv preprint arXiv:2512.02556* (2025).

[80] MiroMind AI Team. *MiroFlow: A High-Performance Open-Source Research Agent Framework*. <https://github.com/MiroMindAI/MiroFlow>. 2025.

- [81] Qihao Zhao et al. “Mmlu-cf: A contamination-free multi-task language understanding benchmark”. In: *Proceedings of the 63rd Annual Meeting of the Association for Computational Linguistics (Volume 1: Long Papers)*. 2025, pp. 13371–13391.
- [82] Adyasha Maharana et al. “Evaluating very long-term conversational memory of llm agents”. In: *arXiv preprint arXiv:2402.17753* (2024).
- [83] Zhongyue Zhang et al. “OriGene: A Self-Evolving Virtual Disease Biologist Automating Therapeutic Target Discovery”. In: *bioRxiv* (2025).
- [84] David Weininger. “SMILES, a chemical language and information system. 1. Introduction to methodology and encoding rules”. In: *Journal of chemical information and computer sciences* 28.1 (1988), pp. 31–36.
- [85] Greg Landrum. “Rdkit documentation”. In: *Release 1.1-79* (2013), p. 4.
- [86] Ondrej Kovar et al. “Scaffold Hopping in Tuberculosis Drug Discovery: Principles, Applications, and Case Studies”. In: *Journal of Medicinal Chemistry* 68.20 (2025), pp. 20903–20929.
- [87] Reiichiro Nakano et al. “Webgpt: Browser-assisted question-answering with human feedback”. In: *arXiv preprint arXiv:2112.09332* (2021).
- [88] Timo Schick et al. “Toolformer: Language models can teach themselves to use tools”. In: *Advances in Neural Information Processing Systems (NeurIPS)* (2023).
- [89] xAI. *Grok-3 DeepSearch: Synthesizing Key Information to Distill Clarity from Complexity*. <https://x.ai/news/grok-3>. 2025.
- [90] Perplexity. *Perplexity Deep Research*. <https://www.perplexity.ai/>. 2025.
- [91] Xiaoxi Li et al. “Search-o1: Agentic search-enhanced large reasoning models”. In: *arXiv preprint arXiv:2501.05366* (2025).
- [92] Zile Qiao et al. “WebResearcher: Unleashing unbounded reasoning capability in Long-Horizon Agents”. In: *arXiv preprint arXiv:2509.13309* (2025).
- [93] Samuel Schmidgall et al. “Agent laboratory: Using llm agents as research assistants”. In: *arXiv preprint arXiv:2501.04227* (2025).
- [94] Zhili Shen et al. “GeAR: Graph-enhanced Agent for Retrieval-augmented Generation”. In: *arXiv preprint arXiv:2412.18431* (2024).
- [95] Wenxuan Shi et al. “Pangu DeepDiver: Adaptive Search Intensity Scaling via Open-Web Reinforcement Learning”. In: *arXiv preprint arXiv:2505.24332* (2025).
- [96] Yuyang Hu et al. “Memory in the Age of AI Agents”. In: *arXiv preprint arXiv:2512.13564* (2025).
- [97] Yuhuai Wu et al. “Memorizing Transformers”. In: *International Conference on Learning Representations*.
- [98] Weizhi Wang et al. “Augmenting language models with long-term memory”. In: *Advances in Neural Information Processing Systems* 36 (2023), pp. 74530–74543.
- [99] Joon Sung Park et al. “Generative agents: Interactive simulacra of human behavior”. In: *Proceedings of the 36th annual ACM symposium on user interface software and technology*. 2023, pp. 1–22.

A. Appendix

A.1. Contributions and Acknowledgments

Lead Authors

Shiyang Feng¹, Runmin Ma¹, Xiangchao Yan¹

Core Authors

Yue Fan¹, Yusong Hu^{1,6}, Songtao Huang^{1,2}, Shuaiyu Zhang^{1,2}, Zongsheng Cao¹, Tianshuo Peng^{1,4}, Jiakang Yuan^{1,2}, Zijie Guo^{1,2}, Zhijie Zhong¹, Shangheng Du^{1,5}, Weida Wang^{1,2}, Jinxin Shi^{1,5}, Yuhao Zhou¹

Contributors

Xiaohan He, Zhiyin Yu, Fangchen Yu, Bihao Zhan, Qihao Zheng, Jiamin Wu, Mianxin Liu, Chi Zhang, Shaowei Hou, Shuya Li, Yankai Jiang, Wenjie Lou, Lilong Wang, Zifu Wang, Jiong Wang, Wanghan Xu, Yue Deng, Dongrui Liu, Yiheng Wang

Scientific Directors

Wenlong Zhang¹, Fenghua Ling¹, Shufei Zhang¹, Xiaosong Wang¹, Shuangjia Zheng³, Xun Huang³, Siqi Sun^{1,2}, Shuyue Hu¹, Peng Ye^{1,4}, Chunfeng Song¹, Bin Wang¹, Conghui He¹, Yihao Liu¹, Xin Li¹, Qibin Hou⁶, Tao Chen², Xiangyu Yue^{1,4}, Bin Wang², Liang He^{1,5}, Dahua Lin¹, Bowen Zhou¹

Corresponding Authors

Bo Zhang¹, zhangbo@pjlab.org.cn

Lei Bai¹, bailei@pjlab.org.cn

Main Affiliations

¹ Shanghai Artificial Intelligence Laboratory

² Fudan University

³ Lingang Laboratory

⁴ The Chinese University of Hong Kong

⁵ East China Normal University

⁶ Nankai University

A.2. Earth Science example

Report Generated All by InternAgent-1.5

The Future of the Atlantic Meridional Overturning Circulation (AMOC): A Review of Mainstream Consensus, Divergent Projections, and the Risk of a 21st-Century Collapse

Introduction

The Atlantic Meridional Overturning Circulation (AMOC) is a large-scale system of ocean currents vital to the global climate system. Characterized by a northward flow of warm, salty surface water and a southward return of cold, deep water, the AMOC acts as a planetary-scale conveyor, transporting an immense quantity of heat—estimated at 1.25 petawatts—toward the high latitudes. This process is a primary reason for the relatively mild climates of the Northern Hemisphere, particularly in Western Europe. Beyond its role in heat redistribution, the AMOC is a crucial pump in global biogeochemical cycles, facilitating the sequestration of atmospheric carbon into the deep ocean and distributing nutrients essential for marine ecosystems.

Given its critical role, the future stability of the AMOC in the face of anthropogenic climate change has become a subject of intense scientific debate and pressing concern. A significant slowdown or collapse would trigger a cascade of severe global consequences, including dramatic cooling across the Northern Hemisphere, a southward shift of the Intertropical Convergence Zone (ITCZ) that would alter tropical rainfall patterns, and accelerated sea-level rise along the U.S. East Coast [1][2][3]. This report addresses the central question of whether the AMOC will cross a critical tipping point in the 21st century. It examines a scientific landscape characterized by a deep-seated conflict: the mainstream consensus, as articulated by the Intergovernmental Panel on Climate Change (IPCC), which projects a gradual weakening, is increasingly challenged by a body of research suggesting the potential for a more abrupt and imminent collapse.

This divergence in projections arises from fundamental uncertainties inherent in the methods used to study the AMOC. The conflict is driven by differing interpretations of evidence from two primary sources: statistical analyses of paleoclimate proxy records,

which suggest early-warning signals may already be present, and simulations from complex physical climate models, which are known to have biases that may artificially enhance AMOC stability. This report synthesizes the current literature to explore this debate in detail. It will first define the AMOC and its significance, then review the mainstream consensus before investigating the divergent evidence for a potential tipping point. Subsequently, it will analyze the sources of these conflicting predictions, detail the potential consequences of an AMOC disruption, and conclude by summarizing the state of the science and outlining future research priorities.

Understanding the AMOC: Definition, Drivers, and Global Significance

The Atlantic Meridional Overturning Circulation (AMOC) is a large-scale system of ocean currents and a primary component of the global thermohaline circulation, often conceptualized as the "global conveyor belt." This section provides a foundational overview of the AMOC, detailing the physical forces that drive its circulation and its multifaceted significance for the global climate and biogeochemical systems.

Definition and Physical Drivers

At its core, the AMOC is characterized by a northward flow of warm, salty surface and intermediate waters in its upper limb, which is balanced by a southward flow of cold, dense water in its deep lower limb. This immense circulatory system is fundamentally powered by density differences that arise from spatial gradients in seawater temperature (thermo) and salinity (haline). While often simplified as a single conveyor, the AMOC is a dynamically complex system sustained by an intricate interplay between thermodynamic processes and mechanical wind forcing. A basin-scale schematic illustrating these limbs, the main deep-water formation sites, and the roles of thermohaline and wind/tidal forcing is shown below.

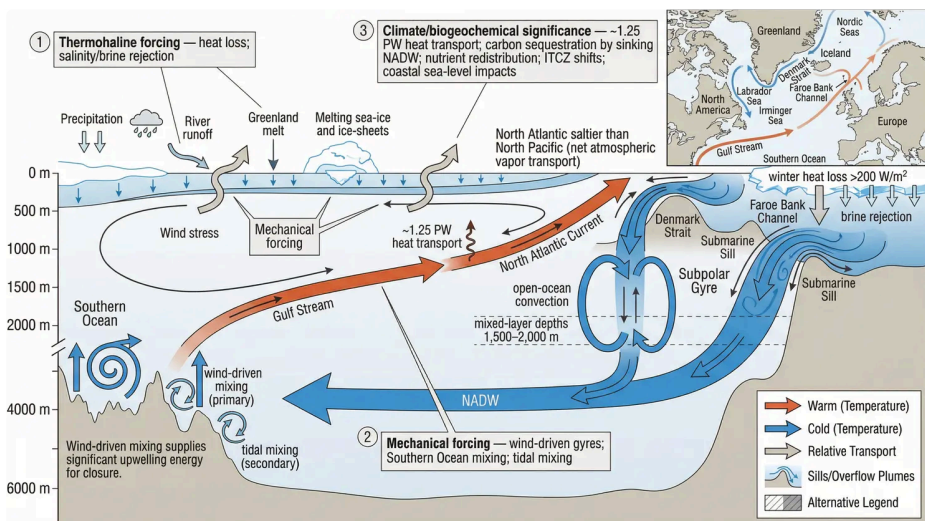


Figure 1. AMOC schematic showing pathways, sinking sites, and thermohaline and wind forcing.

The primary engine of the circulation is **thermohaline forcing**. As warm, highly saline surface waters from the tropics and subtropics are transported northward into the high-latitude North Atlantic, they encounter cold, dry polar air in the Nordic, Greenland, Labrador, and Irminger Seas. This leads to intense atmospheric cooling, with a net heat loss from the ocean that can exceed 200 W/m^2 in winter. This dramatic cooling significantly increases the water's density. The North Atlantic is inherently saltier than the North Pacific—a result of net atmospheric transport of water vapor from the Atlantic to the Pacific basin—which pre-conditions these surface waters, making them more susceptible to sinking upon cooling. The combination of high salinity and extreme cooling makes the surface water gravitationally unstable, causing it to sink to great depths and form North Atlantic Deep Water (NADW). This process of deep-water formation initiates the cold, deep lower limb of the AMOC, which then flows southward, perpetuating the overturning motion.

This density-driven sinking is modulated by **surface buoyancy fluxes**, which encompass the exchange of both heat and freshwater between the ocean and atmosphere. While heat loss is the main driver of densification, freshwater inputs from precipitation, river runoff (e.g., from Greenland), and the melting of sea ice and continental ice sheets can act as a countervailing force. An anomalous influx of freshwater can create a buoyant,

low-salinity lens at the surface, which stratifies the upper water column and can inhibit, or "cap," the deep convection necessary for NADW formation.

Deep-water formation does not occur uniformly across the basin but is concentrated in specific, geographically localized regions. The primary sites include:

1. **The Nordic Seas (Greenland and Norwegian Seas):** Here, densification is intensified by the formation of sea ice, which rejects concentrated brine into the surrounding water, further increasing its salinity and density. This newly formed dense water flows southward over key submarine sills, such as the Denmark Strait and the Faroe Bank Channel, cascading into the North Atlantic basin as dense overflow plumes that entrain surrounding waters and form the deepest components of NADW.
2. **The Subpolar Gyre (Labrador and Irminger Seas):** In this region, a different mode of formation, known as open-ocean convection, occurs. During severe winters, intense cooling and strong winds can erode the seasonal thermocline, mixing the water column to depths of 1,500–2,000 meters. This process forms a slightly less dense variety of NADW. The combined output from these distinct formation sites merges to supply the deep, cold, southward-flowing limb of the AMOC.

While thermohaline processes provide the sinking mechanism, **mechanical forcing from wind stress** is equally critical for sustaining the full AMOC circuit. Wind forcing contributes in two fundamental ways. First, it drives the large-scale horizontal gyre systems, including the powerful Gulf Stream and its eastward extension, the North Atlantic Current. These currents are not separate from the AMOC but are integral to it, efficiently transporting the vast quantities of warm, salty water that fuel the sinking processes in the north. Without this wind-driven transport, the thermohaline engine would be starved of its source waters. Second, the global overturning cell must be closed by the upwelling of deep water back to the surface, and a significant portion of the energy for this vertical movement is supplied by wind-driven mixing, particularly in the Southern Ocean, with smaller contributions from tidal mixing over rough topography. The AMOC must therefore be understood as a hybrid system, where density-driven sinking in the North Atlantic is critically enabled and balanced by wind-driven horizontal transport and global-scale vertical mixing.

Global Climatic and Biogeochemical Significance

The profound global significance of the AMOC stems from its deeply interconnected functions as a planetary-scale heat transporter, a regulator of biogeochemical cycles, and a driver of regional climate.

Its most prominent function is the **redistribution of heat**. By transporting warm surface waters northward, the AMOC's upper limb releases an immense quantity of heat—approximately 1.25 petawatts—to the atmosphere. This heat flux is a primary reason for the relatively mild climates in the Northern Hemisphere, particularly in Western Europe. A substantial weakening or collapse of this heat transport would trigger significant atmospheric cooling across the North Atlantic, fundamentally reshaping continental weather patterns and altering storm tracks.

Beyond its thermodynamic role, the AMOC is a crucial pump in the **global carbon and nutrient cycles**. It facilitates the sequestration of atmospheric carbon dioxide (CO₂) into the deep ocean via both physical and biological mechanisms. The cooling of surface waters at high latitudes increases their capacity to dissolve CO₂, enhancing the ocean's uptake of atmospheric carbon. When these carbon-rich waters sink to form NADW, the carbon is effectively isolated from the atmosphere for centuries to millennia. This mechanism is vital for mitigating the rate of atmospheric CO₂ accumulation and the associated pace of global warming. Concurrently, the overturning circulation is essential for distributing nutrients. The deep, southward-flowing current becomes enriched with nutrients like nitrate and phosphate from the remineralization of sinking organic matter. When this nutrient-laden deep water eventually upwells in other ocean basins, such as the Southern Ocean and equatorial regions, it fertilizes the sunlit surface waters, fueling primary productivity and supporting the base of marine food webs on a global scale. A slowdown of the AMOC would thus diminish the ocean's capacity to act as a carbon sink and disrupt marine ecosystems far from the Atlantic.

Finally, the AMOC directly influences **regional climate phenomena and coastal sea levels** through complex dynamic adjustments and teleconnections. Variations in AMOC strength are strongly correlated with the latitudinal position of the Intertropical Convergence Zone (ITCZ), a critical band of tropical rainfall. A weaker AMOC is associated with a southward shift of the ITCZ, a phenomenon linked to severe and persistent droughts in the African Sahel and alterations to monsoon systems in South America and South Asia, thereby impacting agriculture and water security for billions. Furthermore, the circulation governs Atlantic sea level dynamics. The strong, northward-flowing Gulf Stream, as part of the AMOC's upper limb, maintains a cross-basin pressure gradient that results in a lower sea level along the North American coast compared to the European side. A weakening of this current would cause the gradient to relax, leading to an anomalous and accelerated rate of sea-level rise along the eastern seaboard of the United States, independent of global mean sea-level rise from melting ice. The state of the AMOC also modulates Atlantic hurricane activity by influencing sea surface

temperatures and vertical wind shear, further highlighting its multifaceted impact on climatic hazards.

The Mainstream Consensus: Historical Variability and Projected 21st-Century Weakening

The mainstream scientific consensus, largely articulated in assessments by the Intergovernmental Panel on Climate Change (IPCC), draws a sharp distinction between the AMOC's volatile history and its projected 21st-century trajectory. Paleoclimate evidence reveals a system capable of dramatic and abrupt shifts, particularly during glacial periods, which later settled into a state of relative stability during the Holocene. In stark contrast, analyses of the industrial era and projections for the coming century point toward an anomalous and sustained weakening directly attributed to anthropogenic climate change. While a gradual, progressive decline is a high-confidence projection, the potential for an abrupt collapse before 2100 remains a low-probability, high-impact risk clouded by acknowledged uncertainties in climate modeling.

A Long-Term Perspective: From Glacial Volatility to Holocene Stability

Paleoclimatological reconstructions provide an essential long-term context for understanding AMOC behavior, revealing a system that was far more volatile during the Late Pleistocene (c. 126,000 to 11,700 years ago) than in the current interglacial epoch. The last glacial period was marked by large-scale, rapid climate oscillations known as Dansgaard-Oeschger (D-O) events. The consensus view establishes a direct link between these events and significant fluctuations in AMOC strength. These fluctuations drove a “bipolar seesaw” effect, wherein a strengthened AMOC would transport more heat northward, leading to rapid warming over the North Atlantic and Greenland (by as much as 8–15°C within decades), while the Southern Ocean simultaneously cooled. Conversely, periods of AMOC weakening reversed this pattern. The primary triggers for these abrupt slowdowns are strongly associated with massive freshwater discharges into the North Atlantic originating from collapsing ice sheets (known as Heinrich events) and large meltwater pulses, such as the one that initiated the Younger Dryas cold period approximately 12,800 years ago. This influx of buoyant freshwater stratified the surface ocean, critically inhibiting the deep convection in the Nordic and Labrador Seas that is essential for the formation of North Atlantic Deep Water (NADW) and the overall drive of the overturning circulation [1].

Following the end of the last glacial period, the AMOC transitioned into a comparatively quiescent phase during the Holocene epoch, which began roughly 11,700 years ago. High-resolution sedimentary proxy records, such as the ratio of protactinium-231 to thorium-230 ($^{231}\text{Pa}/^{230}\text{Th}$), support a broad consensus that AMOC variability was significantly subdued compared to the preceding glacial era. These reconstructions suggest that the AMOC recovered from a weak state during the deglaciation period and stabilized to a strength comparable to pre-industrial levels around 6,500 years ago. Despite this general stability, the circulation did not lose its sensitivity to freshwater forcing. A notable weakening event, for instance, is associated with the 8.2 ka climate event—a prominent cooling episode in the Northern Hemisphere linked to the final drainage of proglacial lakes from the Laurentide Ice Sheet. This Holocene record serves to underscore a fundamental property of the AMOC: even within a stable background climate, its strength is fundamentally modulated by changes in the surface buoyancy fluxes of the North Atlantic [1][4].

The Modern Era: Detecting Trends Amidst Natural Fluctuation

Assessing AMOC variability during the instrumental era is fraught with challenges, highlighted by a divergence between short-term direct observations, longer-term proxy reconstructions, and climate model simulations. Continuous, direct monitoring of the AMOC has only been possible since 2004 with the implementation of the RAPID-MOCHA array at 26.5°N. While this invaluable record has documented substantial interannual variability, including a notable temporary 30% decline in 2009–2010, its short duration makes it difficult to definitively isolate a long-term, anthropogenically forced trend from natural, low-frequency oscillations like the Atlantic Multidecadal Oscillation (AMO), which operates on a timescale of roughly 70 years [5].

To extend the record further into the past, scientists rely on proxy-based reconstructions using indicators like sea surface temperature patterns. A growing body of such studies concludes that the AMOC has experienced a significant weakening of 15–20% since the mid-20th century, with some analyses suggesting it is now in its weakest state in over a millennium. The anomalous “cold blob” of surface water observed in the subpolar North Atlantic is interpreted by some researchers as indirect evidence of this reduced northward heat transport [1]. This conclusion, however, is an area of active scientific debate. Other studies have challenged the robustness of these proxy reconstructions, pointing to potentially confounding atmospheric factors that could alternatively explain the observed temperature patterns. This debate underscores the inherent uncertainties in reconstructing a complex, three-dimensional ocean circulation from limited data.

Climate models have historically added another layer of complexity; comprehensive General Circulation Models (GCMs) often simulated a relatively stable AMOC throughout the 20th century, a finding at odds with the weakening trend suggested by proxies. The IPCC's Sixth Assessment Report (AR6), utilizing the latest CMIP6 models, notes that while these models simulate interannual variability, they have struggled to fully capture observed changes and may possess a bias toward excessive stability [6].

Projected 21st-Century Weakening and the Risk of Collapse

Despite the complexities of historical reconstruction, the mainstream scientific consensus, as formally articulated by the IPCC, projects with *very high confidence* that the AMOC will weaken over the course of the 21st century. This conclusion is a robust outcome across nearly all global climate models and under various emissions scenarios. The physical rationale for this slowdown is rooted in fundamental climate principles: anthropogenic global warming leads to intensified surface warming and an increased influx of freshwater into the North Atlantic. This freshwater comes from the accelerating melt of the Greenland Ice Sheet and Arctic sea ice, as well as from changing precipitation patterns. Together, these factors reduce the density of surface waters, enhance ocean stratification, and inhibit the deep-water formation in high-latitude seas that propels the entire circulation [7].

The multi-model ensemble mean from the Coupled Model Intercomparison Project Phase 6 (CMIP6) projects an AMOC decline of 34% to 45% by the year 2100 under high-emissions scenarios (e.g., SSP5-8.5). This corresponds to a transport reduction of approximately 6 to 8 Sverdrups (Sv) and represents a more pronounced weakening than was projected in the previous generation of CMIP5 models [8]. While a considerable spread exists across individual models, with some projecting a more moderate weakening of up to 30%, the general agreement across different modeling frameworks reinforces the core consensus of a significant slowdown [9].

A critical distinction within this consensus lies between a gradual weakening and a potential abrupt collapse. The IPCC's Special Report on the Ocean and Cryosphere in a Changing Climate (SROCC) and its Sixth Assessment Report (AR6) both assess an abrupt AMOC collapse before 2100 as *very unlikely*. However, the IPCC qualifies this assessment with only *medium confidence*, a crucial caveat that reflects acknowledged model limitations and the profound, catastrophic impacts such an event would entail [10][11]. This confidence level signifies that while a collapse is not the expected outcome this century, the possibility cannot be entirely ruled out. The decision to lower the confidence

level from *high* (in AR5) to *medium* (in AR6) was partly informed by growing evidence of the system's modern instability [6]. This uncertainty is largely rooted in recognized biases within climate models, which may be inherently predisposed to excessive AMOC stability and thus underestimate its sensitivity to freshwater forcing—the very mechanism implicated in past abrupt changes. Specific structural biases identified in CMIP6 models include an underrepresentation of the deep-water transport component known as Lower North Atlantic Deep Water (INADW) and coarse model resolutions that limit the accurate simulation of critical processes like deep-water overflows and narrow boundary currents [12]. This divergence between the gradual decline projected by most comprehensive models and the more imminent tipping points suggested by some statistical analyses underscores that the future of the AMOC remains a critical and active area of climate research [13]. As summarized in Table 1, key IPCC assessments, model projections, confidence levels, drivers, and primary uncertainties are organized for quick reference.

Table 1: Summary of IPCC projections, collapse risk, confidence levels, drivers, and model uncertainties

Aspect	Summary	Quantitative projection / magnitude	AR6 confidence	AR5 confidence
Projected 21st-century weakening	With very high confidence, the AMOC will weaken over the course of the 21st century; a gradual, progressive decline is a robust outcome across nearly all global climate models and emissions scenarios.	CMIP6 multi-model ensemble mean: ~34–45% decline by 2100 under high-emissions scenarios (SSP5-8.5), corresponding to ~6–8 Sv transport reduction; some models project a more moderate weakening (~30%).	Very high confidence	Not specified
Abrupt collapse before 2100	An abrupt AMOC collapse before 2100 is assessed as very unlikely; however, this remains a low-probability, high-impact risk that cannot be fully ruled out.	Probability: very unlikely (IPCC AR6); characterized as low-probability, high-impact.	Medium confidence (that collapse before 2100 is very unlikely)	High confidence (collapse very unlikely)
Confidence level comparison (AR6 vs AR5)	AR6 assigns very high confidence to projected weakening, but lowers confidence that an abrupt collapse before 2100 is very unlikely compared with AR5.	Confidence change: collapse confidence reduced from “high” (AR5) to “medium” (AR6).	Very high (weakening); Medium (collapse very unlikely)	High (collapse very unlikely)

Aspect	Key drivers	Primary uncertainties / model biases	Notes / sources
Projected 21st-century weakening	Anthropogenic global warming; intensified surface warming; increased freshwater input from Greenland Ice Sheet and Arctic sea-ice melt; altered precipitation patterns reducing surface-water density and inhibiting North Atlantic Deep Water (NADW) formation.	Limited instrumental record (continuous RAPID-MOCHA observations since 2004); proxy reconstruction uncertainties; climate-model biases toward excessive AMOC stability; underrepresentation of Lower North Atlantic Deep Water (LNADW); coarse resolution limiting representation of deep-water overflows and boundary currents.	IPCC AR6; CMIP6 multi-model results; references cited in text (e.g., [7], [8], [6]).
Abrupt collapse before 2100	Paleoclimate analogues: massive freshwater discharges from collapsing ice sheets (Heinrich events) and large meltwater pulses (e.g., Younger Dryas); contemporary drivers include accelerating Greenland melt, Arctic sea-ice loss, and increased precipitation-driven stratification.	Structural model limitations may underestimate collapse risk; excessive AMOC stability bias; limited representation of LNADW; coarse spatial resolution; short observational record; emerging evidence of modern AMOC instability.	IPCC AR6 and SROCC assessments; discussion in text (e.g., [10], [11], [6]).

Primary drivers and uncertainties (synthesis)	Anthropogenic warming and freshwater forcing dominate long-term weakening; abrupt changes historically linked to extreme freshwater perturbations.	Proxy-model disagreement; limited observations; known structural and resolution-related model biases affecting AMOC sensitivity to freshwater forcing.	Paragraph references for drivers and uncertainties (e.g., [1], [4], [5], [6], [12]).
---	--	--	--

The Tipping Point Debate: Divergent Evidence for an Imminent Collapse

While the mainstream consensus from large-scale climate modeling efforts, such as the Coupled Model Intercomparison Project Phase 6 (CMIP6), largely projects a gradual weakening of the Atlantic Meridional Overturning Circulation (AMOC) through the 21st century without a full collapse, a significant and growing body of research presents a starkly different conclusion. These studies suggest that the AMOC may be much closer to a critical tipping point, with an abrupt transition plausible within decades rather than centuries [1][14]. This divergence from the prevailing view stems from two primary, and increasingly intersecting, lines of investigation that challenge the stability inherent in many Earth System Models (ESMs). The first relies on statistical analyses of observational and paleoclimate data to detect early-warning signals (EWS) of an impending critical transition. The second leverages specialized climate models, designed to overcome stability biases, to identify physically-based precursors to collapse, which are then sought in observationally-constrained datasets.

Statistical Early-Warning Signals in Observational and Paleoclimate Data

The most compelling argument for an approaching AMOC collapse is rooted in the statistical analysis of time-series data, which applies the theoretical framework of dynamical systems nearing a critical transition. According to this theory, as a complex system like the AMOC loses resilience, it exhibits a phenomenon known as 'critical slowing down' (CSD). This process, where the system's recovery rate from minor perturbations diminishes, produces detectable statistical fingerprints, most notably an increase in variance and lag-1 autocorrelation (AR1) [10].

A prominent 2023 study by Ditlevsen applied this framework to sea surface temperature (SST) data from the subpolar gyre, a region whose thermal properties are dynamically coupled to AMOC heat transport and can serve as an effective proxy. The analysis uncovered a statistically significant increase in both variance and autocorrelation in the SST record, with the trend accelerating notably since the 1970s. By extrapolating these trends based on the theoretical behavior of a system approaching a saddle-node bifurcation, the study produced an alarming forecast: an AMOC collapse is most likely to occur mid-century, with a 95% confidence interval spanning 2025–2095 and a central estimate around 2057 [10]. As illustrated in Figure 2, the collapse timing estimates and their associated uncertainties diverge sharply between the different methodologies of statistical EWS analyses, specialized model experiments, and the broader CMIP6 ensembles.

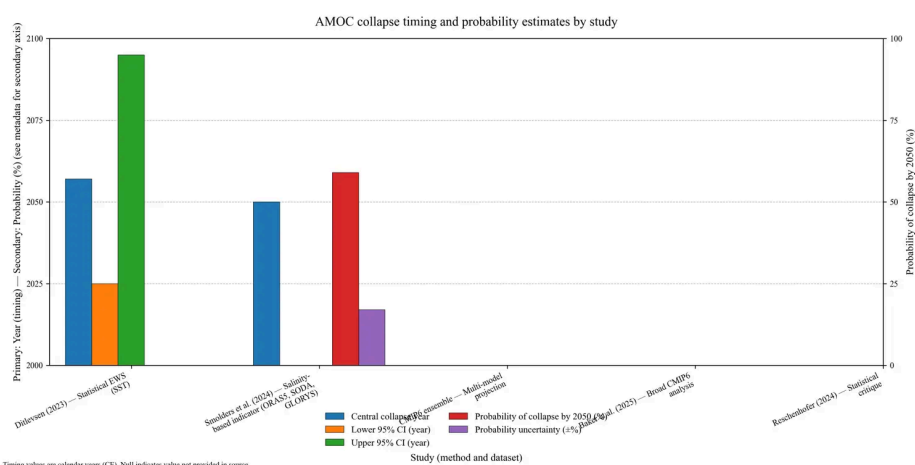


Figure 2. Horizontal comparison of AMOC collapse timing and probability estimates.

This statistical evidence is corroborated by research seeking to reconcile observed signals with model behavior. Shin et al. (2025) identified a consistent warning signal—increasing AR1 of both SST and salinity—in the eastern Subpolar North Atlantic (SPNA). A crucial finding of their work is that while ESMs can produce these signals, they only do so under future warming scenarios that far exceed Paris Agreement targets. The fact that these EWS are already present in observational records under current climate conditions strongly implies that ESMs may systematically overestimate AMOC stability. The study directly links these statistical signals to physical oceanographic changes, pointing to a significant freshening event in the eastern SPNA between 2014 and 2019 as empirical

evidence of a critical decline in stability driven by freshwater flux [15]. The validity of using such statistical indicators is further bolstered by paleoclimate evidence. As mentioned previously, the AMOC is a known tipping element responsible for past abrupt climate shifts, such as Dansgaard-Oeschger events [16]. Moreover, a 2022 analysis by Michel et al. of thousand-year-long paleoclimate reconstructions confirmed that rising autoregressive properties served as detectable EWS for past climatic transitions in the North Atlantic, lending strong theoretical and historical credence to applying these methods to modern observational data [17].

Physically-Based Precursors from Specialized Models

A second, pivotal line of evidence bridges the gap between idealized model physics and real-world observations. This approach uses specialized model experiments to identify an optimal, physically-based EWS that is more robust than purely statistical indicators. A 2024 simulation using the Community Earth System Model (CESM) successfully induced a classic AMOC collapse by applying a gradual but sustained influx of freshwater to the North Atlantic over 1,700 years. Although the magnitude of the forcing required was considered unrealistically high, this was deemed a necessary measure to counteract the model's intrinsic stability bias. The primary achievement of this experiment was not to predict the timing of collapse but to identify a robust physical precursor: the strength of the southward freshwater transport at the Atlantic's southern boundary (34°S) [1].

Building directly upon this model-derived insight, Smolders et al. (2024) used this specific salinity-based indicator to analyze several ocean reanalysis datasets—ORAS5, SODA, and GLORYS—which integrate vast observational data into a dynamically consistent framework. Their analysis detected a pronounced CSD pattern in the southward freshwater transport, particularly at depths below 500 meters along the 34°S transect. By extrapolating the observed decline in the system's restoring rate, the study produced a startling forecast that directly contradicts the low-probability, post-2100 collapse assessments from the IPCC and most CMIP6 models. They calculated a mean collapse time of 2050, with a 59% ($\pm 17\%$) probability of the tipping event occurring before that year [18].

Methodological Debates and Countervailing Evidence

The stark projections from studies like Ditlevsen (2023) and Smolders et al. (2024) have ignited significant scientific debate, with scrutiny focused on both the statistical methods and the fidelity of the climate models themselves. In a direct critique, Reschenhofer

(2024) argues that the statistical techniques used to detect CSD, particularly the use of rolling windows on short and potentially non-stationary time series, lack robustness. Citing a structural break in the data in the late 1990s that could invalidate the core assumptions of EWS methods, Reschenhofer applied an alternative statistical approach (a Hodrick-Prescott filter and cumulative plotting) to the same reanalysis data and found no evidence of an impending collapse. This alternative analysis showed no trend towards a minimum in freshwater transport and no sign of increasing variance or autocorrelation [19].

On the modeling front, the apparent stability of most CMIP6 models is itself a subject of intense discussion. There is a growing concern that this stability might be an artifact of shared model deficiencies, such as the misrepresentation of freshwater transport pathways that artificially divert freshwater away from the critical deep-water formation zones in the North Atlantic [1]. Indeed, studies have shown that a model previously stable under a CO₂-doubling scenario can be induced to collapse after 300 years once such biases are corrected. Furthermore, when CMIP6 simulations are extended beyond 2100 under high-emissions scenarios, a consensus for collapse does emerge; one analysis found that all nine models examined exhibited a complete shutdown of the deep northern overturning cell, confirming that a tipping point is a consistent feature of these models, albeit on a longer timescale [1].

However, other model-based analyses reveal powerful countervailing factors that could promote AMOC stability. Research by Sinet et al. (2025) demonstrated that meltwater from the West Antarctic Ice Sheet can exert a stabilizing influence, potentially counteracting or even preventing a collapse induced by meltwater from the Greenland Ice Sheet [20]. In a broad analysis of 34 CMIP6 models, Baker et al. (2025) concluded that a 21st-century collapse is unlikely, pointing to robust stabilizing feedbacks, such as wind-driven upwelling in the Southern Ocean, that sustain the global overturning circuit [14]. This highlights the central conflict in the current scientific landscape: while tailored statistical and model-based analyses designed to detect tipping points suggest a proximate threat, broader suites of climate models indicate a system with powerful, though perhaps not insurmountable, resilience.

Sources of Divergence: Biases in Paleoclimate Proxies and Climate Models

The substantial divergence in scientific predictions regarding the 21st-century stability of the Atlantic Meridional Overturning Circulation (AMOC) is rooted in fundamental

challenges and biases inherent in the two primary methodologies used for its study: the statistical analysis of paleoclimate proxies and simulations with complex climate models. While proxies provide a crucial long-term perspective, their interpretation is fraught with uncertainty, leading to conflicting assessments of past variability and the presence of early-warning signals (EWS). Conversely, while climate models offer a physically-based framework for future projections, many contain systemic biases that may artificially enhance AMOC stability, masking its true vulnerability. This section examines these sources of divergence, first by detailing the limitations of paleoclimate reconstructions and then by analyzing systemic errors within climate models.

Challenges in Statistical Analyses of Paleoclimate Proxies

The wide spectrum of conclusions drawn from paleoclimate records—from forecasts of imminent collapse to findings of relative stability—stems from a cascade of issues related to data quality, interpretation, and statistical methodology. These challenges begin with the proxies themselves, which are indirect, noisy, and geographically limited representations of the vast and complex AMOC system [21].

Inherent Proxy Limitations and Signal Ambiguity: A foundational constraint is the limited spatial and temporal resolution of proxy archives. Data from a single sediment or ice core provides point-based information that can be dominated by local or regional climate variability, potentially masking or mimicking a basin-scale AMOC signal [21]. Furthermore, the temporal resolution of key archives like marine sediment cores, where a single data point may represent an average over decades or centuries, is often too coarse to resolve the high-frequency changes in variance and autocorrelation that are hallmarks of critical slowing down, a key theoretical basis for EWS [21]. The integrity of the climate signal is also frequently compromised by processes within the archive. Bioturbation in marine sediments, for instance, acts as a low-pass filter, which can artificially increase autocorrelation and generate a spurious EWS that is an artifact of the archive, not a true climate signal [22]. Hiatuses, changes in sediment focusing, signal diffusion, and layer thinning in ice cores can further corrupt the fidelity of the record [22] [23].

Perhaps the most significant source of conflicting interpretations is that most proxies respond to multiple environmental factors. For example, foraminiferal $\delta^{18}\text{O}$ is a composite signal reflecting sea temperature, global ice volume, and local salinity. A change in this proxy could be plausibly attributed to an AMOC-induced temperature shift, a meltwater signal from the Greenland Ice Sheet, or a local freshening event, allowing

different research teams to arrive at divergent conclusions from the same data [24]. Similarly, while alkenone-based sea surface temperatures (SSTs) are more direct, a temperature change in the subpolar gyre is still a combined result of AMOC heat transport, atmospheric patterns, and local gyre dynamics [10][24].

Uncertainties in Data Interpretation and Reconstruction: The process of converting raw proxy data into a time series introduces further uncertainty. The construction of an age model to establish a chronology is an inherently uncertain process, with error margins in methods like radiocarbon dating. An inaccurate age model that stretches or compresses time can artificially create or obscure statistical trends in EWS metrics like lag-1 autocorrelation (AR1), which are highly sensitive to the temporal spacing of data points [25]. Likewise, the calibration of a proxy measurement to a physical variable like SST is a statistical exercise where the choice of model (e.g., simple linear regression vs. complex Bayesian models) can yield different reconstructions [26]. A critical issue is the frequent underestimation of uncertainty from the calibration process itself; if the "unexplained variance" is not rigorously propagated, the resulting time series may appear deceptively precise, biasing EWS analysis by masking significant fluctuations [26]. This culminates in the central challenge of separating a faint EWS signal from a dominant noise background, which is often "red" noise possessing its own autocorrelation that can be indistinguishable from a genuine EWS [10][17][27].

The Role of Methodological Assumptions: The final and most dramatic source of divergence lies in the statistical methods applied to the reconstructed time series. The search for EWS is governed by assumptions that can predetermine the outcome. For instance, the theoretical framework often assumes stationarity, but climate records contain long-term forcings and abrupt shifts (structural breaks) that can be misinterpreted by a rolling-window analysis as a simultaneous increase in variance and autocorrelation, creating a "phantom" EWS [19]. The choice of detrending method to address this—from a rigid linear fit to a flexible Gaussian kernel—creates a trade-off where one might leave artifacts (false positives) and the other might remove the genuine signal (false negatives) [19]. The selection of the primary indicator (e.g., subpolar gyre SSTs vs. southward freshwater transport) also preconditions the outcome [1][10]. Perhaps most significantly, alarming predictions of a collapse within a specific timeframe (e.g., 2025-2095) are not derived solely from observing a trend but from fitting that trend to a specific theoretical model of a system approaching a bifurcation, such as a saddle-node bifurcation [10]. This powerful assumption allows for extrapolation to a precise collapse point, but the conclusion is entirely conditional on the chosen model being correct. This methodological leap explains the vast gulf between studies forecasting an

imminent collapse and those analyzing the same underlying data to find no significant trend at all [19][10].

Biases and Uncertainties in Complex Climate Models

Divergence in AMOC projections also arises from fundamental biases and incomplete physics within the complex climate models used for forecasting. While large-scale efforts like the Coupled Model Intercomparison Project Phase 6 (CMIP6) generally project a gradual AMOC weakening without an abrupt collapse, this apparent consensus on stability is increasingly scrutinized as a potential artifact of shared model deficiencies, particularly in the representation of freshwater feedbacks and cryospheric interactions [1].

Intrinsic Stability Biases from Misrepresented Feedbacks: A critical source of artificial AMOC stability in many Earth System Models (ESMs) is a systemic misrepresentation of the salt-advection feedback. The stability of the AMOC is governed by the meridional freshwater transport by the overturning circulation, quantified as F_{ovS} . Observational data indicate F_{ovS} is negative, signifying a net freshwater export that creates a positive, destabilizing feedback. However, a majority of CMIP models erroneously simulate a positive F_{ovS} , implying a net freshwater import. This inverts the sign of a key feedback, hard-wiring an artificial stability into the model climate that dampens its response to perturbations [28]. This bias is deeply embedded, as even high-resolution models initialized in a more realistic state eventually drift toward the biased, positive F_{ovS} regime [28].

The origin of this pervasive bias is often teleconnected to remote processes, particularly a systematic positive freshwater flux bias over the Indian Ocean. In many models, excessive precipitation in this region creates an anomalously fresh surface layer that is transported into the South Atlantic via the Agulhas Leakage. This influx artificially freshens the entire Atlantic basin, contributing to the erroneous positive F_{ovS} and making the modeled AMOC more resilient to freshening from North Atlantic sources like Greenland meltwater [28][29]. Bifurcation analyses confirm that this remote bias shifts the AMOC's collapse threshold to an "unrealistic parameter regime," which explains why many CMIP6 models appear stable and require unrealistically high freshwater forcing to induce a collapse in experimental settings. When such freshwater transport biases are corrected, a previously stable model can be made to collapse under more realistic forcing levels [1].

Divergence from Incomplete Ocean-Ice Sheet Interactions: Significant divergence also stems from how models represent the complex and often competing feedbacks from melting ice sheets. The transition from idealized “hosing” experiments with prescribed freshwater forcing to fully coupled, dynamic ice sheet models has revealed critical new dynamics [1]. For instance, meltwater from the Antarctic Ice Sheet (AIS) can introduce a powerful delaying effect on AMOC decline. Under a high-emissions scenario, AIS discharge can lead to profound cooling in the Southern Ocean and an expansion of sea ice. This powerful negative feedback counteracts anthropogenic warming and, through climatic teleconnections, slows the rate of AMOC change in the Northern Hemisphere, potentially delaying a projected collapse by approximately 35 years [30]. Models lacking this dynamic coupling are therefore likely to produce more pessimistic near-term stability assessments.

Complicating this further, meltwater from different poles can exert opposing influences. While Greenland Ice Sheet (GIS) melt is a well-documented destabilizing agent, meltwater from the West Antarctic Ice Sheet (WAIS) can have a stabilizing effect, increasing the AMOC's resilience to GIS-induced freshening [20]. A model's projection is therefore exquisitely sensitive to the relative timing and magnitude of melt from each pole; models that focus predominantly on GIS melt will invariably identify a more vulnerable AMOC [20]. Finally, a foundational uncertainty lies in how models generate and route meltwater. Basal melting, driven by geothermal heat flux, represents a continuous freshwater source that is often omitted or inadequately parameterized [31]. Furthermore, meltwater is often distributed uniformly over large ocean grid cells in models, whereas in reality, it is channeled through subglacial networks to specific points. These differences in the spatial distribution and depth of freshwater injection can profoundly alter the local oceanic response, particularly stratification in critical deep-water formation regions, creating another axis of divergence in AMOC projections [30].

Potential Consequences of an AMOC Disruption

A significant slowdown or complete collapse of the Atlantic Meridional Overturning Circulation (AMOC) would not be a singular event but would instead precipitate a cascade of profound, interconnected, and globally significant consequences. As a primary engine for the planetary redistribution of heat, nutrients, and carbon, the AMOC's stability is intrinsically linked to regional temperature regimes, hydrological cycles, and the biogeochemical functioning of the world's oceans. A disruption would induce a complex and regionally heterogeneous reorganization of Earth's systems,

underscoring the critical importance of resolving the scientific debate surrounding its future trajectory.

Climatic Reorganization and Atmospheric Dynamics

The most direct consequence of a substantial AMOC slowdown is a dramatic thermal rebalancing between the hemispheres. The circulation is responsible for transporting an estimated 1.25 petawatts of heat poleward, which moderates the climate of the North Atlantic region. A collapse would disrupt this heat transport, inducing severe cooling across the Northern Hemisphere, with a particular concentration in Northwestern Europe. Model projections indicate an average surface air temperature drop of 3.4°C in Great Britain and between 4°C and 10°C across parts of Northern Europe. Some simulations suggest that winter cooling could be as extreme as 10°C to 30°C within a century, creating conditions where winter sea ice could extend into the territorial waters of the British Isles and Denmark [1][32]. This would create a distinctive regional cooling pattern, often referred to as the North Atlantic "cold blob," in stark contrast to the background signal of global warming. Concurrently, as this heat is no longer transported north, a slight warming is expected in the Southern Hemisphere, a phenomenon known as the "bipolar seesaw" [1][32].

The impacts of this thermal reorganization would extend far beyond the North Atlantic. Climate models indicate the emergence of a "climatic dipole" in South America, where tropical regions would experience cooling while extratropical areas to the south would face warming and increased aridity [2][33]. The same AMOC weakening that cools Europe is projected to cause more frequent and intense summer heatwaves in South America's La Plata Basin [33]. The magnitude of these climatic shifts is strongly linked to the degree of AMOC decline; models simulating a more moderate weakening project a pattern of minimum warming in the subpolar North Atlantic rather than absolute cooling, highlighting the AMOC's state as a major source of uncertainty in regional climate projections [2].

A weakened AMOC would also fundamentally restructure global precipitation patterns, primarily by causing a southward shift of the Intertropical Convergence Zone (ITCZ), the planet's main tropical rain belt, a teleconnection mentioned in previous sections. This atmospheric response occurs because the AMOC's northward heat transport helps to position the ITCZ farther north; a weakening of the circulation relaxes this pull. This southward displacement, a classic signature of a weakened AMOC observed in paleoclimate records from periods like the Younger Dryas, would trigger severe and

persistent droughts in regions such as the African Sahel and lead to a significant reduction in average rainfall and snowfall over Europe and the mid-latitudes, threatening water security for millions [1][3]. This atmospheric reorganization creates a complex mosaic of effects. While some regions would face drought, Northeast Brazil is projected to receive more intense extreme precipitation events, and increased rainfall over the southern Amazon could potentially counteract forest dieback trends [2]. The AMOC's influence extends to global monsoon systems as well; a slowdown is expected to alter the Indian Monsoon, and variability in the AMOC's South Atlantic component (SAMOC) has been shown to modulate monsoon intensity with a lead time of 15-20 years [34]. Furthermore, altered atmospheric pressure and temperature gradients would reconfigure storm tracks. Projections from the IPCC and other studies suggest a potential strengthening of the North Atlantic storm track. One controversial hypothesis posits that a full collapse could dramatically increase the thermal gradient between the cold subpolar region and its surroundings, fueling more powerful mid-latitude cyclonic "superstorms" with near-hurricane-force winds in winter [1].

Environmental and Biogeochemical Consequences

The AMOC's disruption would also have a direct, dynamic impact on regional sea levels. As discussed previously, the strong northward flow of the Gulf Stream maintains a pressure gradient across the Atlantic. A slowdown of this current would cause this gradient to relax, triggering an anomalous and accelerated rate of sea-level rise along the U.S. East Coast that is distinct from, and additive to, global mean sea-level rise [2].

Furthermore, the AMOC is a crucial component of the global carbon cycle. As previously outlined, it acts as a vital pump that sequesters atmospheric CO₂ when warm surface waters cool and sink in the high-latitudes, effectively isolating carbon in the deep ocean for centuries to millennia [35]. A slowdown would severely diminish this sequestration capacity, leaving more anthropogenic CO₂ in the atmosphere and creating a positive feedback loop that exacerbates global warming. This reduction in ocean carbon uptake, termed the "AMOC carbon feedback," is projected to range from 7.5 to 32 petagrams of carbon (PgC) by 2100. Studies indicate a quasi-linear reduction of approximately 0.2 PgC per year for every 10 Sverdrup (Sv) decline in AMOC strength, with potentially trillions of dollars in unaccounted-for climate damages and an aggravation of ocean acidification [36][35].

The AMOC is also essential for distributing the nutrients that support marine life. The deep, southward-flowing limb of the circulation, which becomes enriched with nitrate

and phosphate from sinking organic matter, transports this vital supply to other basins where it upwells and fertilizes surface waters [2]. A disruption would sever this critical nutrient supply chain, leading to a significant decrease in primary productivity. This would have cascading effects through the food web, affecting zooplankton populations and the stocks of commercially vital fish like cod and haddock, triggering a large-scale reorganization of marine habitats and threatening biodiversity [36].

Finally, the AMOC is engaged in a complex feedback loop with the cryosphere. While freshwater from melting ice sheets is a primary driver of AMOC weakening, the state of the AMOC in turn influences ice sheet stability [37]. Meltwater from the West Antarctic Ice Sheet, for example, can have a dual effect, potentially preventing, facilitating, or even triggering a recovery of the AMOC depending on the specific characteristics of the freshwater influx. This highlights the risk of cascading tipping events where the stability of the Greenland Ice Sheet, the West Antarctic Ice Sheet, and the AMOC are coupled. While a full collapse within this century is considered unlikely, a significant weakening of 20-81% is deemed possible under extreme scenarios, with these non-linear interactions representing a major source of uncertainty in climate projections [14][37].

Conclusion and Future Research Priorities

The stability of the Atlantic Meridional Overturning Circulation (AMOC) in the 21st century remains a subject of significant scientific debate and uncertainty. The current body of research is characterized by a fundamental divergence: while many comprehensive Earth System Models (ESMs) project a gradual, non-critical weakening, a growing number of studies using paleoclimate proxies and statistical analyses of observational data suggest a critical tipping point could be crossed this century. This report has synthesized the evidence underpinning these conflicting views, revealing that the divergence stems from deep-seated limitations in both modeling and observational approaches. To reconcile these findings and produce a more reliable, uncertainty-quantified assessment of AMOC risk, a comprehensive research strategy is imperative. Future priorities must be directed towards systematically addressing the weaknesses in both domains, enhancing the fidelity of past reconstructions and improving the physical realism of future projections [1].

The specific limitations inherent to each methodology, and the research required to address them, are summarized in Table 2.

Table 2: Comparison of paleoclimate reconstructions and climate models/ESMs, their biases, and recommended fixes

Category	Primary Inputs/Processes	Typical Limitations/Biases	Consequences for AMOC Inference	Recommended Methodological Fixes
Paleoclimate Reconstruction	Paleoclimate proxy records from sediment and ice cores (e.g., foraminiferal $\delta^{18}\text{O}$), data archives, statistical methods for EWS detection, age models, calibration methods.	Geographically sparse and temporally coarse records; bias from local variability masking basin-scale signals. Post-depositional artifacts (bioturbation) generating spurious EWS. Age model uncertainties creating or erasing trends. Calibration methods underestimating variance and noise. Non-stationarity and structural breaks misinterpreted as EWS.	Interpretive ambiguity; risk of incorrect conclusions from artifacts. Distorted trend detection from age model errors. Difficulty distinguishing faint EWS from complex "red noise" backgrounds. Overly alarming predictions from simplified model extrapolations.	Expand high-resolution core archives in key regions. Develop and validate novel circulation proxies. Use multi-proxy reconstructions to disentangle drivers. Use integrated Bayesian chronological modeling to propagate age uncertainty. Develop and validate EWS algorithms robust to non-stationarity.

Climate Models/ESMs	<p>Earth System Models (ESMs) with physical oceanography, cryospheric interactions, salt-advection feedback, air-sea fluxes, and ice sheet dynamics.</p>	<p>Artificial AMOC stability from misrepresented salt-advection feedback (erroneous positive F_{ovS}), often linked to remote biases (e.g., Indian Ocean precipitation). Omission of dynamic Antarctic melt and its stabilizing teleconnections. Underestimation of total freshwater budgets (e.g., omitting basal melting). Oversimplified meltwater routing (uniform distribution).</p>	<p>AMOC is rendered overly resilient to perturbations. Projections of vulnerability are biased and incomplete. Localized impact of meltwater on stratification and deep convection is underestimated.</p>	<p>Improve atmospheric parameterization to eliminate remote freshwater biases. Use higher-resolution models for inter-basin exchange. Validate physical realism of feedback loops (sign/magnitude of F_{ovS}). Implement fully coupled, two-way interactive ice sheet models for both poles in all major modeling projects. Develop and implement high-resolution subglacial hydrology and plume models for realistic meltwater routing.</p>
----------------------------	--	--	---	---

Advancing Paleoclimate Reconstructions of AMOC Variability

Improving the empirical foundation for AMOC behavior requires a concerted effort to enhance the quality and interpretation of paleoclimate proxy records. This involves improving data archives, refining analytical frameworks, and developing more robust statistical methods for detecting early-warning signals (EWS).

First, to move beyond divergent conclusions rooted in geographically sparse and temporally coarse records, a critical priority is to expand the paleoclimatic archive network. Existing records can be biased by local variability that may either mask or mimic a true basin-scale AMOC signal, underscoring the need for new, high-resolution sediment and ice cores from dynamically significant regions like deep-water formation zones [21]. Concurrently, research must focus on developing and validating novel proxies that offer more direct measurements of circulation, moving beyond traditional indicators like foraminiferal $\delta^{18}\text{O}$ that conflate temperature, ice volume, and salinity effects [24]. The adoption of multi-proxy reconstructions is essential for reducing this interpretive ambiguity [10][24]. Furthermore, non-climatic noise within archives—such as bioturbation or discontinuities from submarine landslides—can generate spurious EWS [22][23]. A key research avenue is the development of proxy system and diagenetic models to quantify and correct for these post-depositional artifacts [22].

Second, the interpretive frameworks that translate raw proxy measurements into a time series must be fundamentally improved. To address the profound uncertainty introduced by age models—where errors in temporal spacing can create or erase EWS trends—future work must prioritize integrated Bayesian chronological modeling techniques that allow for robust propagation of age-model uncertainty [25]. Similarly, proxy calibration methods must rigorously account for all sources of uncertainty. Many reconstructions differ due to choices in calibration and the underestimation of “unexplained variance” [26]. Research should shift towards protocols, such as hierarchical Bayesian models, that produce probabilistic ensembles of time series rather than single “best-fit” reconstructions [27]. Such ensembles are crucial for realistically assessing the signal-to-noise ratio and distinguishing a faint EWS from the complex “red noise” background inherent to paleoclimatic data [10][17].

Third, the statistical methodologies used for EWS detection must be made more robust. As current methods can misinterpret abrupt “structural breaks” in non-stationary records as “phantom” EWS, a priority is to develop and validate detection algorithms robust to these conditions, benchmarking them against synthetic data and ESM output where the ground truth is known [19]. The selection of analytical parameters, such as

detrending methods, must become more objective and data-driven [19]. Confidence in any detected signal would be increased by a shift to multi-indicator approaches, seeking EWS consistently across different proxies representing distinct components of the AMOC system [1][10]. Finally, the field must bridge the gap between statistical trend detection and physical forecasting. Instead of relying on simplified bifurcation models for extrapolation, future work should develop integrated frameworks that provide probabilistic risk assessments, conditioning any forecast on deep uncertainties and using physics-based models for plausible constraints [10].

Refining Climate Model Projections of AMOC Stability

To scrutinize the apparent consensus on 21st-century AMOC resilience—a consensus that may be an artifact of shared model deficiencies—research must address systemic biases in model physics and cryospheric interactions [1].

First, a paramount priority is to correct fundamental model biases that artificially stabilize the AMOC. The most critical of these is the misrepresentation of the salt-advection feedback. A majority of ESMs erroneously simulate a net meridional freshwater import into the Atlantic (a positive F_{ovS}), which inverts the sign of a key destabilizing feedback and renders the model AMOC overly resilient. In contrast, observations indicate a net freshwater export (a negative F_{ovS}), implying a positive, self-reinforcing feedback [29]. As this bias is often teleconnected to remote processes like excessive precipitation over the Indian Ocean, future work must improve atmospheric parameterizations and use higher-resolution ocean models to resolve inter-basin exchange [28]. New validation protocols are needed to assess the realism of such feedback loops. Systematically performing bifurcation analyses on ESMs is also essential to reveal whether a model's stability is genuine or an artifact of biases [29][38].

Second, the representation of ocean-ice sheet interactions must be significantly advanced. A crucial priority is to accelerate the transition from idealized freshwater “hosing” experiments to the universal implementation of fully coupled, two-way interactive ice sheet models for both Greenland and Antarctica. This is essential because meltwater from different poles can exert opposing influences. While Greenland Ice Sheet (GIS) melt is a known destabilizing agent, recent modeling shows that Antarctic Ice Sheet (AIS) melt can induce a powerful stabilizing feedback by cooling the Southern Ocean, which through teleconnections can delay an AMOC collapse by decades [30]. Melt from the West Antarctic Ice Sheet (WAIS) in particular may increase AMOC resilience to GIS freshening [20]. Since the net effect is sensitive to the relative melt from each pole, future

model intercomparison projects must mandate simulations with fully coupled, bi-hemispheric cryosphere components to avoid incomplete and biased projections [1][20].

Third, the physical realism of how meltwater is generated and routed must be improved. Current models often underestimate the total freshwater budget by omitting sources like basal melting driven by geothermal heat flux, a continuous process largely absent from climate projections [31]. Furthermore, meltwater is often distributed uniformly over vast ocean grid cells, diluting its impact on stratification. In reality, melt is discharged at specific, localized points. Consequently, a key objective is to develop and implement high-resolution subglacial hydrology and plume models that can realistically route meltwater from the ice bed to the ocean, enabling a more accurate assessment of its impact on the local convective processes that drive the AMOC [30].

References

- [1] ● Atlantic meridional overturning circulation - https://en.wikipedia.org/wiki/Atlantic_meridional_overturning_circulation
- [2] ● How a Weakening Atlantic Ocean Circulation Is Rewriting ... - <https://ocean2climate.org/2025/12/28/how-a-weakening-atlantic-current-is-rewriting-south-americas-weather/>
- [3] ● [Commentary] The risk of a potential circulation change in ... - <https://india.mongabay.com/2024/11/commentary-the-risk-of-a-potential-circulation-change-in-the-atlantic-adds-to-climate-worries/>
- [4] ● Low variability of the Atlantic Meridional Overturning ... - <https://www.nature.com/articles/s41467-025-61793-z>
- [5] ● Recent Progress in Understanding and Predicting Atlantic ... - <https://pmc.ncbi.nlm.nih.gov/articles/PMC6991968/>
- [6] ● Figure 3.30 - <https://www.ipcc.ch/report/ar6/wg1/figures/chapter-3/figure-3-30/>
- [7] ● Summary for Policymakers — Special Report on the Ocean ... - <https://www.ipcc.ch/srocc/chapter/summary-for-policymakers/>
- [8] ● CMIP6 Models Predict Significant 21st Century Decline of ... - <https://repository.library.noaa.gov/view/noaa/30634>
- [9] ● Atlantic Ocean Current Expected to Undergo Limited ... - <https://ese.caltech.edu/news/atlantic-ocean-current-expected-to-undergo-limited-weakening-with-climate-change>

- [10] ● Warning of a forthcoming collapse of the Atlantic ... - <https://www.nature.com/articles/s41467-023-39810-w>
- [11] ● expert reaction to paper warning of a collapse of the ... - <https://www.sciencemediacentre.org/expert-reaction-to-paper-warning-of-a-collapse-of-the-atlantic-meridional-overturning-circulation/>
- [12] ● Comparing observed and modelled components of the ... - OS - <https://os.copernicus.org/articles/20/589/2024/>
- [13] ● Substantial Risk of 21st Century AMOC Tipping even under ... - <https://arxiv.org/ht/ml/2407.19909v1>
- [14] ● Continued Atlantic overturning circulation even under ... - <https://www.nature.com/articles/s41586-024-08544-0>
- [15] 📄 Reconciled warning signals in observations and models imply approaching AMOC tipping point - <https://arxiv.org/pdf/2503.22111v1>
- [16] ● FEATURE ARTICLE • Is the Atlantic Overturning Circulation ... - <https://tos.org/oceanography/article/is-the-atlantic-overturning-circulation-approaching-a-tipping-point>
- [17] ● Early warning signal for a tipping point suggested by a ... - <https://pmc.ncbi.nlm.nih.gov/articles/PMC9440003/>
- [18] 📄 Probability Estimates of a 21st Century AMOC Collapse - <https://arxiv.org/pdf/2406.11738v1>
- [19] 📄 A new indicator for the AMOC strength still gives no indication of an imminent collapse - <https://arxiv.org/pdf/2402.16600v1>
- [20] 📄 West Antarctic Meltwater can Prevent an AMOC Collapse - <https://arxiv.org/pdf/2502.17104v1>
- [21] ● Global and regional sea-surface temperature changes over ... - <https://cp.copernicus.org/articles/21/1895/2025/>
- [22] ● Sustained North Atlantic warming drove anomalously intense ... - <https://pmc.ncbi.nlm.nih.gov/articles/PMC11251152/>
- [23] ● Multi-proxy constraints on Atlantic circulation dynamics ... - <https://pmc.ncbi.nlm.nih.gov/articles/PMC10089918/>
- [24] ● δ 18 O water isotope in the iLOVECLIM model (version ... - <https://gmd.copernicus.org/articles/6/1505/2013/gmd-6-1505-2013-relations.html>

- [25] ● Quantifying age and model uncertainties in palaeoclimate ... - <https://pmc.ncbi.nlm.nih.gov/articles/PMC6501663/>
- [26] ● Statistical Uncertainty in Paleoclimate Proxy Reconstructions - <https://pubmed.ncbi.nlm.nih.gov/35860010/>
- [27] ● Simple noise estimates and pseudoproxies for the last 21 ... - <https://essd.copernicus.org/articles/11/1129/>
- [28] ● Persistent climate model biases in the Atlantic Ocean's ... - OS - <https://os.copernicus.org/articles/20/549/2024/>
- [29] ● [2308.11751] The effect of model freshwater flux biases on ... - <https://arxiv.org/abs/2308.11751>
- [30] ● Antarctic ice sheet - climate feedbacks under high future carbon emissions - [http://arxiv.org/pdf/2005.09731v1](https://arxiv.org/pdf/2005.09731v1)
- [31] ● Liquid Water on Cold Exo-Earths via Basal Melting of Ice Sheets - <https://arxiv.org/pdf/2212.03702v1>
- [32] ● Revisiting climate impacts of an AMOC slowdown - [https://pmc.ncbi.nlm.nih.gov/articles/PMC11578178/](https://pmc.ncbi.nlm.nih.gov/articles/PMC11578178)
- [33] ● Future climate change shaped by inter-model differences ... - <https://www.nature.com/articles/s41467-021-24015-w>
- [34] ● Atlantic Meridional Overturning Circulation and Its Impact ... - https://www.aoml.noaa.gov/phod/research/moc/moc_monsoons/index.php
- [35] ● Weakening AMOC reduces ocean carbon uptake and ... - <https://pmc.ncbi.nlm.nih.gov/articles/PMC11892582/>
- [36] ● How Does AMOC Affect Marine Life? → Question - <https://climate.sustainability-directory.com/question/how-does-amoc-affect-marine-life/>
- [37] ● Meltwater from West Antarctic ice sheet tipping affects ... - <https://pmc.ncbi.nlm.nih.gov/articles/PMC12617517/>
- [38] ● Physics of AMOC multistable regime shifts due to freshwater ... - <https://esd.copernicus.org/articles/16/1221/2025/>